



Wind-energy generator farm, Altamont Pass, California. Windmills have been used for power for more than two thousand years. These multi-bladed horizontal-axis wind turbines (HAWT's) are among the most efficient of windpower designs, as discussed in this chapter. *(Courtesy of Kevin Schafer/Peter Arnold, Inc.)*

Chapter 11

Turbomachinery

Motivation. The most common practical engineering application for fluid mechanics is the design of fluid machinery. The most numerous types are machines which *add* energy to the fluid (the pump family), but also important are those which *extract* energy (turbines). Both types are usually connected to a rotating shaft, hence the name *turbomachinery*.

The purpose of this chapter is to make elementary engineering estimates of the performance of fluid machines. The emphasis will be upon nearly incompressible flow, i.e., liquids or low-velocity gases. Basic flow principles are discussed, but not the detailed construction of the machine.

11.1 Introduction and Classification

Turbomachines divide naturally into those which add energy (pumps) and those which extract energy (turbines). The prefix *turbo-* is a Latin word meaning “spin” or “whirl,” appropriate for rotating devices.

The pump is the oldest fluid-energy-transfer device known. At least two designs date before Christ: (1) the undershot-bucket waterwheels, or *norias*, used in Asia and Africa (1000 B.C.) and (2) Archimedes’ screw pump (250 B.C.), still being manufactured today to handle solid-liquid mixtures. Paddlewheel turbines were used by the Romans in 70 B.C., and Babylonian windmills date back to 700 B.C. [1].

Machines which deliver liquids are simply called *pumps*, but if gases are involved, three different terms are in use, depending upon the pressure rise achieved. If the pressure rise is very small (a few inches of water), a gas pump is called a *fan*; up to 1 atm, it is usually called a *blower*; and above 1 atm it is commonly termed a *compressor*.

Classification of Pumps

There are two basic types of pumps: positive-displacement and dynamic or momentum-change pumps. There are several billion of each type in use in the world today.

Positive-displacement pumps (PDPs) force the fluid along by volume changes. A cavity opens, and the fluid is admitted through an inlet. The cavity then closes, and the fluid is squeezed through an outlet. The mammalian heart is a good example, and many mechanical designs are in wide use. The text by Warring [14] gives an excellent summary of PDPs. A brief classification of PDP designs is as follows:

- A. Reciprocating
 - 1. Piston or plunger
 - 2. Diaphragm
- B. Rotary
 - 1. Single rotor
 - a. Sliding vane
 - b. Flexible tube or lining
 - c. Screw
 - d. Peristaltic (wave contraction)
 - 2. Multiple rotors
 - a. Gear
 - b. Lobe
 - c. Screw
 - d. Circumferential piston

All PDPs deliver a pulsating or periodic flow as the cavity volume opens, traps, and squeezes the fluid. Their great advantage is the delivery of any fluid regardless of its viscosity.

Figure 11.1 shows schematics of the operating principles of seven of these PDPs. It is rare for such devices to be run backward, so to speak, as turbines or energy extractors, the steam engine (reciprocating piston) being a classic exception.

Since PDPs compress mechanically against a cavity filled with liquid, a common feature is that they develop immense pressures if the outlet is shut down for any reason. Sturdy construction is required, and complete shutoff would cause damage if pressure-relief valves were not used.

Dynamic pumps simply add momentum to the fluid by means of fast-moving blades or vanes or certain special designs. There is no closed volume: The fluid increases momentum while moving through open passages and then converts its high velocity to a pressure increase by exiting into a diffuser section. Dynamic pumps can be classified as follows:

- A. Rotary
 - 1. Centrifugal or radial exit flow
 - 2. Axial flow
 - 3. Mixed flow (between radial and axial)
- B. Special designs
 - 1. Jet pump or ejector (see Fig. P3.36)
 - 2. Electromagnetic pumps for liquid metals
 - 3. Fluid-actuated: gas-lift or hydraulic-ram

We shall concentrate in this chapter on the rotary designs, sometimes called *rotodynamic pumps*. Other designs of both PDP and dynamic pumps are discussed in specialized texts [for example, 11, 14, 31].

Dynamic pumps generally provide a higher flow rate than PDPs and a much steadier discharge but are ineffective in handling high-viscosity liquids. Dynamic pumps also generally need *priming*; i.e., if they are filled with gas, they cannot suck up a liquid from below into their inlet. The PDP, on the other hand, is self-priming for most

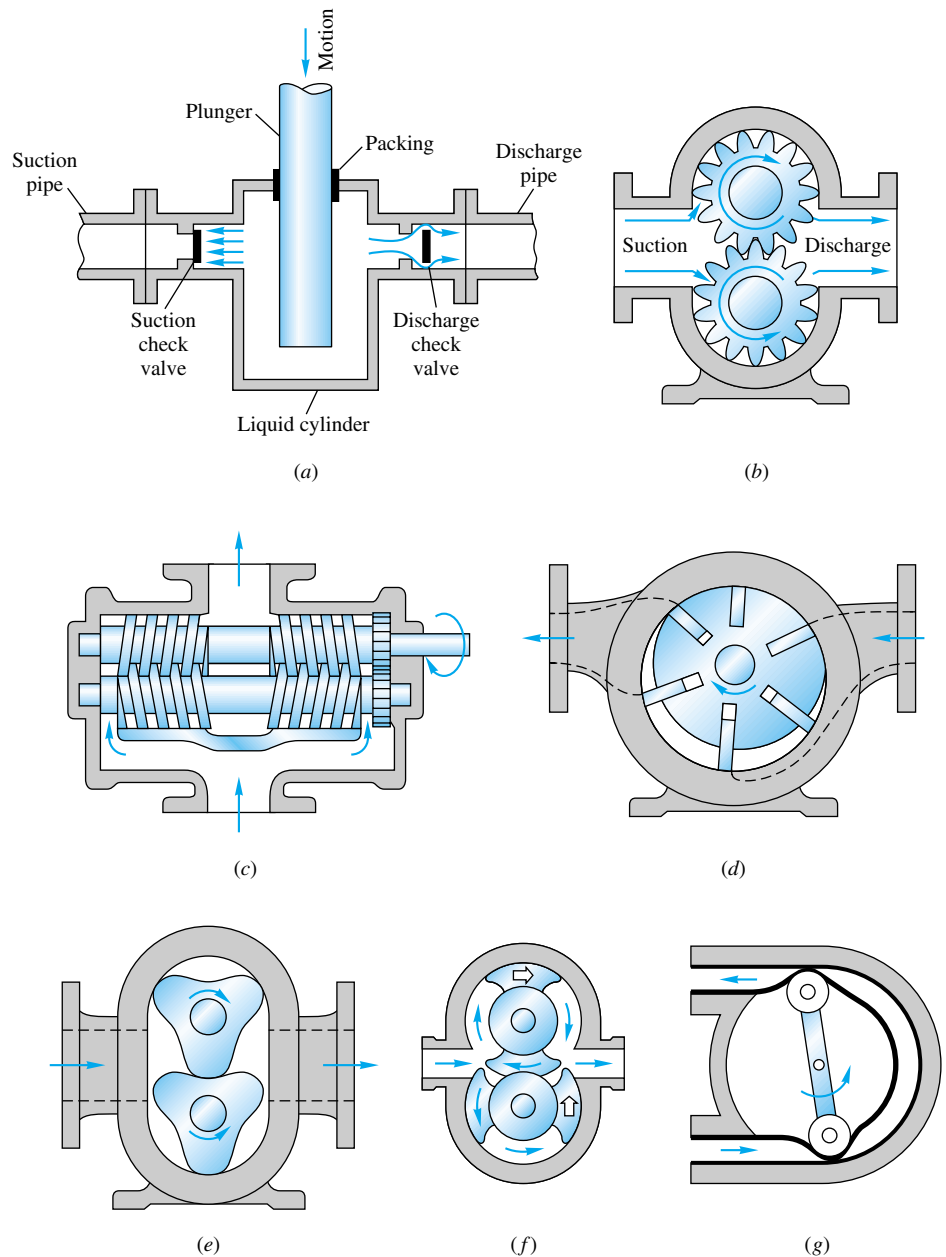


Fig. 11.1 Schematic design of positive-displacement pumps: (a) reciprocating piston or plunger, (b) external gear pump, (c) double-screw pump, (d) sliding vane, (e) three-lobe pump, (f) double circumferential piston, (g) flexible-tube squeegee.

applications. A dynamic pump can provide very high flow rates (up to 300,000 gal/min) but usually with moderate pressure rises (a few atmospheres). In contrast, a PDP can operate up to very high pressures (300 atm) but typically produces low flow rates (100 gal/min).

The relative performance (Δp versus Q) is quite different for the two types of pump, as shown in Fig. 11.2. At constant shaft rotation speed, the PDP produces nearly con-

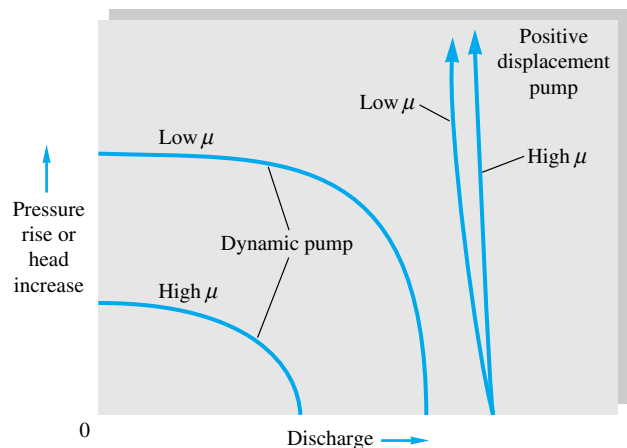


Fig. 11.2 Comparison of performance curves of typical dynamic and positive-displacement pumps at constant speed.

stant flow rate and virtually unlimited pressure rise, with little effect of viscosity. The flow rate of a PDP cannot be varied except by changing the displacement or the speed. The reliable constant-speed discharge from PDPs has led to their wide use in metering flows [35].

The dynamic pump, by contrast in Fig. 11.2, provides a continuous constant-speed variation of performance, from near-maximum Δp at zero flow (shutoff conditions) to zero Δp at maximum flow rate. High-viscosity fluids sharply degrade the performance of a dynamic pump.

As usual—and for the last time in this text—we remind the reader that this is merely an introductory chapter. Many books are devoted solely to turbomachines: generalized treatments [2 to 7], texts specializing in pumps [8 to 16], fans [17 to 20], compressors [21 to 23], turbines [24 to 28], and PDPs [35 to 38]. There are several useful handbooks [29 to 32], and at least two elementary textbooks [33, 34] have a comprehensive discussion of turbomachines. The reader is referred to these sources for further details.

11.2 The Centrifugal Pump

Let us begin our brief look at rotodynamic machines by examining the characteristics of the centrifugal pump. As sketched in Fig. 11.3, this pump consists of an impeller rotating within a casing. Fluid enters axially through the *eye* of the casing, is caught

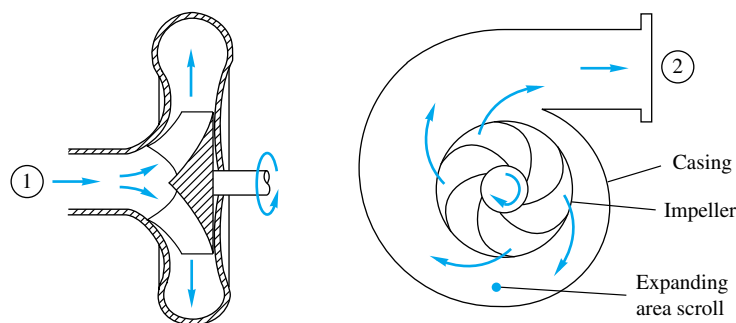


Fig. 11.3 Cutaway schematic of a typical centrifugal pump.

up in the impeller blades, and is whirled tangentially and radially outward until it leaves through all circumferential parts of the impeller into the diffuser part of the casing. The fluid gains both velocity and pressure while passing through the impeller. The doughnut-shaped diffuser, or *scroll*, section of the casing decelerates the flow and further increases the pressure.

The impeller blades are usually *backward-curved*, as in Fig. 11.3, but there are also radial and forward-curved blade designs, which slightly change the output pressure. The blades may be *open*, i.e., separated from the front casing only by a narrow clearance, or *closed*, i.e., shrouded from the casing on both sides by an impeller wall. The diffuser may be *vaneless*, as in Fig. 11.3, or fitted with fixed vanes to help guide the flow toward the exit.

Basic Output Parameters

Assuming steady flow, the pump basically increases the Bernoulli head of the flow between point 1, the eye, and point 2, the exit. From Eq. (3.67), neglecting viscous work and heat transfer, this change is denoted by H :

$$H = \left(\frac{p}{\rho g} + \frac{V^2}{2g} + z \right)_2 - \left(\frac{p}{\rho g} + \frac{V^2}{2g} + z \right)_1 = h_s - h_f \quad (11.1)$$

where h_s is the pump head supplied and h_f the losses. The net head H is a primary output parameter for any turbomachine. Since Eq. (11.1) is for incompressible flow, it must be modified for gas compressors with large density changes.

Usually V_2 and V_1 are about the same, $z_2 - z_1$ is no more than a meter or so, and the net pump head is essentially equal to the change in pressure head

$$H \approx \frac{p_2 - p_1}{\rho g} = \frac{\Delta p}{\rho g} \quad (11.2)$$

The power delivered to the fluid simply equals the specific weight times the discharge times the net head change

$$P_w = \rho g Q H \quad (11.3)$$

This is traditionally called the *water horsepower*. The power required to drive the pump is the *brake horsepower*¹

$$\text{bhp} = \omega T \quad (11.4)$$

where ω is the shaft angular velocity and T the shaft torque. If there were no losses, P_w and brake horsepower would be equal, but of course P_w is actually less, and the *efficiency* η of the pump is defined as

$$\eta = \frac{P_w}{\text{bhp}} = \frac{\rho g Q H}{\omega T} \quad (11.5)$$

The chief aim of the pump designer is to make η as high as possible over as broad a range of discharge Q as possible.

¹ Conversion factors may be needed: 1 hp = 550 ft · lbf/s = 746 W.

The efficiency is basically composed of three parts: volumetric, hydraulic, and mechanical. The *volumetric efficiency* is

$$\eta_v = \frac{Q}{Q + Q_L} \quad (11.6)$$

where Q_L is the loss of fluid due to leakage in the impeller-casing clearances. The *hydraulic efficiency* is

$$\eta_h = 1 - \frac{h_f}{h_s} \quad (11.7)$$

where h_f has three parts: (1) *shock* loss at the eye due to imperfect match between inlet flow and the blade entrances, (2) *friction* losses in the blade passages, and (3) *circulation* loss due to imperfect match at the exit side of the blades.

Finally, the *mechanical efficiency* is

$$\eta_m = 1 - \frac{P_f}{\text{bhp}} \quad (11.8)$$

where P_f is the power loss due to mechanical friction in the bearings, packing glands, and other contact points in the machine.

By definition, the total efficiency is simply the product of its three parts

$$\eta \equiv \eta_v \eta_h \eta_m \quad (11.9)$$

The designer has to work in all three areas to improve the pump.

Elementary Pump Theory

You may have thought that Eqs. (11.1) to (11.9) were formulas from pump *theory*. Not so; they are merely definitions of performance parameters and cannot be used in any predictive mode. To actually *predict* the head, power, efficiency, and flow rate of a pump, two theoretical approaches are possible: (1) simple one-dimensional-flow formulas and (2) complex digital-computer models which account for viscosity and three-dimensionality. Many of the best design improvements still come from testing and experience, and pump research remains a very active field [39]. The last 10 years have seen considerable advances in *computational fluid-dynamics* (CFD) modeling of flow in turbomachines [42], and at least eight commercial turbulent-flow three-dimensional CFD codes are now available.

To construct an elementary theory of pump performance, we assume one-dimensional flow and combine idealized fluid-velocity vectors through the impeller with the angular-momentum theorem for a control volume, Eq. (3.55).

The idealized velocity diagrams are shown in Fig. 11.4. The fluid is assumed to enter the impeller at $r = r_1$ with velocity component w_1 tangent to the blade angle β_1 plus circumferential speed $u_1 = \omega r_1$ matching the tip speed of the impeller. Its absolute entrance velocity is thus the vector sum of w_1 and u_1 , shown as V_1 . Similarly, the flow exits at $r = r_2$ with component w_2 parallel to the blade angle β_2 plus tip speed $u_2 = \omega r_2$, with resultant velocity V_2 .

We applied the angular-momentum theorem to a turbomachine in Example 3.14 (Fig. 3.13) and arrived at a result for the applied torque T

$$T = \rho Q (r_2 V_{t2} - r_1 V_{t1}) \quad (11.10)$$

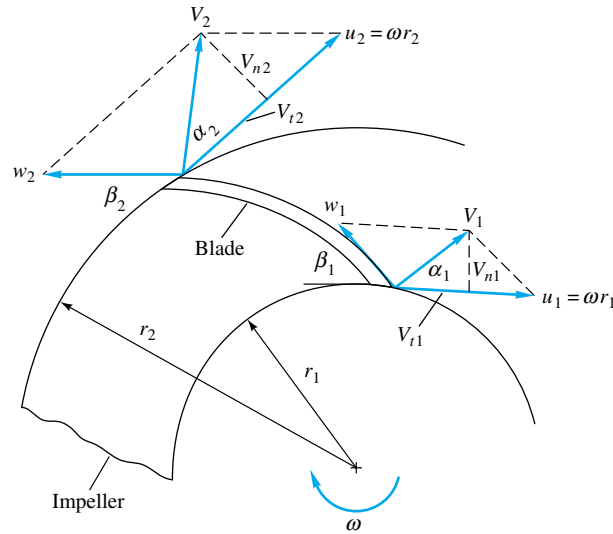


Fig. 11.4 Inlet and exit velocity diagrams for an idealized pump impeller.

where V_{t1} and V_{t2} are the absolute circumferential velocity components of the flow. The power delivered to the fluid is thus

$$P_w = \omega T = \rho Q(u_2 V_{t2} - u_1 V_{t1})$$

or

$$H = \frac{P_w}{\rho g Q} = \frac{1}{g} (u_2 V_{t2} - u_1 V_{t1}) \quad (11.11)$$

These are the *Euler turbomachine equations*, showing that the torque, power, and ideal head are functions only of the rotor-tip velocities $u_{1,2}$ and the absolute fluid tangential velocities $V_{t1,2}$, independent of the axial velocities (if any) through the machine.

Additional insight is gained by rewriting these relations in another form. From the geometry of Fig. 11.4

$$V^2 = u^2 + w^2 - 2uw \cos \beta \quad w \cos \beta = u - V_t$$

or

$$u V_t = \frac{1}{2}(V^2 + u^2 - w^2) \quad (11.12)$$

Substituting this into Eq. (11.11) gives

$$H = \frac{1}{2g} [(V_2^2 - V_1^2) + (u_2^2 - u_1^2) - (w_2^2 - w_1^2)] \quad (11.13)$$

Thus the ideal head relates to the absolute plus the relative kinetic-energy change of the fluid minus the rotor-tip kinetic-energy change. Finally, substituting for H from its definition in Eq. (11.1) and rearranging, we obtain the classic relation

$$\frac{p}{\rho g} + z + \frac{w^2}{2g} - \frac{r^2 \omega^2}{2g} = \text{const} \quad (11.14)$$

This is the *Bernoulli equation in rotating coordinates* and applies to either two- or three-dimensional ideal incompressible flow.

For a centrifugal pump, the power can be related to the radial velocity $V_n = V_t \tan \alpha$ and the continuity relation

$$P_w = \rho Q(u_2 V_{n2} \cot \alpha_2 - u_1 V_{n1} \cot \alpha_1) \quad (11.15)$$

where

$$V_{n2} = \frac{Q}{2\pi r_2 b_2} \quad \text{and} \quad V_{n1} = \frac{Q}{2\pi r_1 b_1}$$

and where b_1 and b_2 are the blade widths at inlet and exit. With the pump parameters r_1 , r_2 , β_1 , β_2 , and ω known, Eqs. (11.11) or Eq. (11.15) is used to compute idealized power and head versus discharge. The “design” flow rate Q^* is commonly estimated by assuming that the flow enters exactly normal to the impeller

$$\alpha_1 = 90^\circ \quad V_{n1} = V_1 \quad (11.16)$$

We can expect this simple analysis to yield estimates within ± 25 percent for the head, water horsepower, and discharge of a pump. Let us illustrate with an example.

EXAMPLE 11.1

Given are the following data for a commercial centrifugal water pump: $r_1 = 4$ in, $r_2 = 7$ in, $\beta_1 = 30^\circ$, $\beta_2 = 20^\circ$, speed = 1440 r/min. Estimate (a) the design-point discharge, (b) the water horsepower, and (c) the head if $b_1 = b_2 = 1.75$ in.

Solution

Part (a) The angular velocity is $\omega = 2\pi \text{ r/s} = 2\pi(1440/60) = 150.8 \text{ rad/s}$. Thus the tip speeds are $u_1 = \omega r_1 = 150.8(4/12) = 50.3 \text{ ft/s}$ and $u_2 = \omega r_2 = 150.8(7/12) = 88.0 \text{ ft/s}$. From the inlet-velocity diagram, Fig. E11.1a, with $\alpha_1 = 90^\circ$ for design point, we compute

$$V_{n1} = u_1 \tan 30^\circ = 29.0 \text{ ft/s}$$

whence the discharge is

$$\begin{aligned} Q &= 2\pi r_1 b_1 V_{n1} = (2\pi) \left(\frac{4}{12} \right) \left(\frac{1.75}{12} \right) (29.0) \\ &= (8.87 \text{ ft}^3/\text{s})(60 \text{ s/min}) \left(\frac{1728}{231} \text{ gal/ft}^3 \right) \\ &= 3980 \text{ gal/min} \end{aligned}$$

Ans. (a)

(The actual pump produces about 3500 gal/min.)

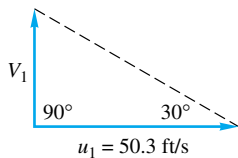
Part (b) The outlet radial velocity follows from Q

$$V_{n2} = \frac{Q}{2\pi r_2 b_2} = \frac{8.87}{2\pi \left(\frac{7}{12} \right) (1.75/12)} = 16.6 \text{ ft/s}$$

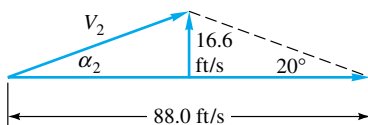
This enables us to construct the outlet-velocity diagram as in Fig. E11.1b, given $\beta_2 = 20^\circ$. The tangential component is

$$V_{t2} = u_2 - V_{n2} \cot \beta_2 = 88.0 - 16.6 \cot 20^\circ = 42.4 \text{ ft/s}$$

$$\alpha_2 = \tan^{-1} \frac{16.6}{42.4} = 21.4^\circ$$



E11.1a



E11.1b

The power is then computed from Eq. (11.11) with $V_{t1} = 0$ at the design point

$$P_w = \rho Q u_2 V_{t2} = (1.94 \text{ slugs/ft}^3)(8.87 \text{ ft}^3/\text{s})(88.0 \text{ ft/s})(42.4 \text{ ft/s})$$

$$= \frac{64,100 \text{ ft} \cdot \text{lb/s}}{550} = 117 \text{ hp} \quad \text{Ans. (b)}$$

(The actual pump delivers about 125 water horsepower, requiring 147 bhp at 85 percent efficiency.)

Part (c) Finally, the head is estimated from Eq. (11.11)

$$H \approx \frac{P_w}{\rho g Q} = \frac{64,100 \text{ ft} \cdot \text{lb/s}}{(62.4 \text{ lbf/ft}^3)(8.87 \text{ ft}^3/\text{s})} = 116 \text{ ft} \quad \text{Ans. (c)}$$

(The actual pump develops about 140-ft head.) Improved methods for obtaining closer estimates are given in advanced references [for example, 6, 8, and 31].

Effect of Blade Angle on Pump Head

The simple theory above can be used to predict an important blade-angle effect. If we neglect inlet angular momentum, the theoretical water horsepower is

$$P_w = \rho Q u_2 V_{t2} \quad (11.17)$$

where
$$V_{t2} = u_2 - V_{n2} \cot \beta_2 \quad V_{n2} = \frac{Q}{2\pi r_2 b_2}$$

Then the theoretical head from Eq. (11.11) becomes

$$H \approx \frac{u_2^2}{g} - \frac{u_2 \cot \beta_2}{2\pi r_2 b_2 g} Q \quad (11.18)$$

The head varies linearly with discharge Q , having a shutoff value u_2^2/g , where u_2 is the exit blade-tip speed. The slope is negative if $\beta_2 < 90^\circ$ (backward-curved blades) and positive for $\beta_2 > 90^\circ$ (forward-curved blades). This effect is shown in Fig. 11.5 and is accurate only at low flow rates.

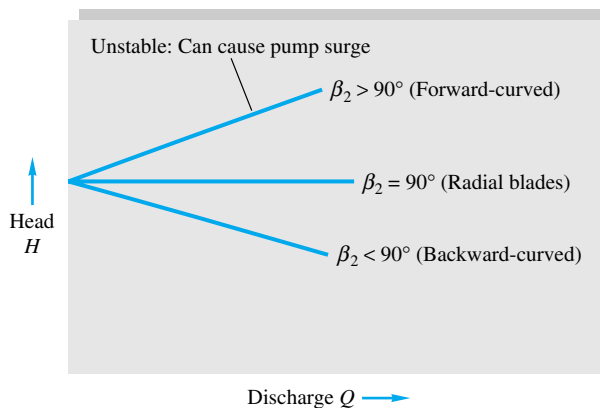


Fig. 11.5 Theoretical effect of blade exit angle on pump head versus discharge.

The measured shutoff head of centrifugal pumps is only about 60 percent of the theoretical value $H_0 = \omega^2 r_2^2 / g$. With the advent of the laser-doppler anemometer, researchers can now make detailed three-dimensional flow measurements inside pumps and can even animate the data into a movie [40].

The positive-slope condition in Fig. 11.5 can be unstable and can cause pump *surge*, an oscillatory condition where the pump “hunts” for the proper operating point. Surge may cause only rough operation in a liquid pump, but it can be a major problem in gas-compressor operation. For this reason a backward-curved or radial blade design is generally preferred. A survey of the problem of pump stability is given by Greitzer [41].

11.3 Pump Performance Curves and Similarity Rules

Since the theory of the previous section is rather qualitative, the only solid indicator of a pump’s performance lies in extensive testing. For the moment let us discuss the centrifugal pump in particular. The general principles and the presentation of data are exactly the same for mixed-flow and axial-flow pumps and compressors.

Performance charts are almost always plotted for constant shaft-rotation speed n (in r/min usually). The basic independent variable is taken to be discharge Q (in gal/min usually for liquids and ft^3/min for gases). The dependent variables, or “output,” are taken to be head H (pressure rise Δp for gases), brake horsepower (bhp), and efficiency η .

Figure 11.6 shows typical performance curves for a centrifugal pump. The head is approximately constant at low discharge and then drops to zero at $Q = Q_{\max}$. At this speed and impeller size, the pump cannot deliver any more fluid than Q_{\max} . The positive-slope part of the head is shown dashed; as mentioned earlier, this region can be unstable and can cause hunting for the operating point.

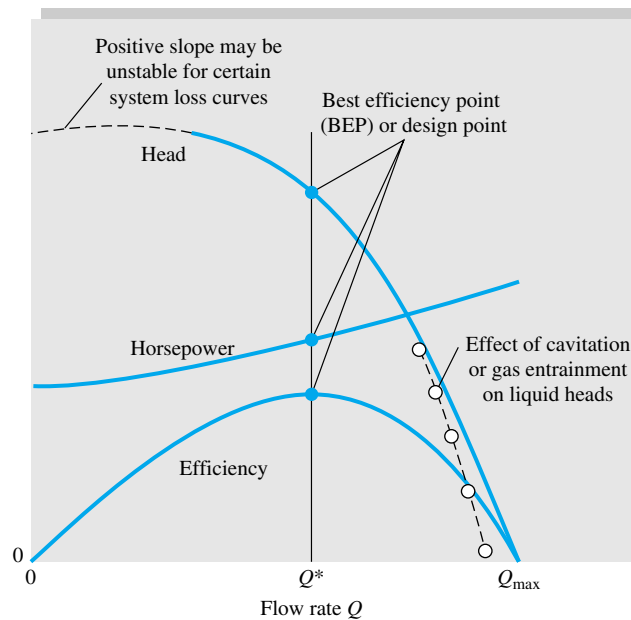


Fig. 11.6 Typical centrifugal pump performance curves at constant impeller-rotation speed. The units are arbitrary.

The efficiency η is always zero at no flow and at Q_{\max} , and it reaches a maximum, perhaps 80 to 90 percent, at about $0.6Q_{\max}$. This is the *design flow rate* Q^* or *best efficiency point* (BEP), $\eta = \eta_{\max}$. The head and horsepower at BEP will be termed H^* and P^* (or bhp^*), respectively. It is desirable that the efficiency curve be flat near η_{\max} , so that a wide range of efficient operation is achieved. However, some designs simply do not achieve flat efficiency curves. Note that η is not independent of H and P but rather is calculated from the relation in Eq. (11.5), $\eta = \rho g Q H / P$.

As shown in Fig. 11.6, the horsepower required to drive the pump typically rises monotonically with the flow rate. Sometimes there is a large power rise beyond the BEP, especially for radial-tipped and forward-curved blades. This is considered undesirable because a much larger motor is then needed to provide high flow rates. Backward-curved blades typically have their horsepower level off above BEP (“nonoverloading” type of curve).

Measured Performance Curves

Figure 11.7 shows actual performance data for a commercial centrifugal pump. Figure 11.7a is for a basic casing size with three different impeller diameters. The head curves $H(Q)$ are shown, but the horsepower and efficiency curves have to be inferred from the contour plots. Maximum discharges are not shown, being far outside the normal operating range near the BEP. Everything is plotted raw, of course [feet, horsepower, gallons per minute (1 U.S. gal = 231 in³)] since it is to be used directly by designers. Figure 11.7b is the same pump design with a 20 percent larger casing, a lower speed, and three larger impeller diameters. Comparing the two pumps may be a little confusing: The larger pump produces exactly the same discharge but only half the horsepower and half the head. This will be readily understood from the scaling or similarity laws we are about to formulate.

A point often overlooked is that raw curves like Fig. 11.7 are strictly applicable to a fluid of a certain density and viscosity, in this case water. If the pump were used to deliver, say, mercury, the brake horsepower would be about 13 times higher while Q , H , and η would be about the same. But in that case H should be interpreted as feet of *mercury*, not feet of water. If the pump were used for SAE 30 oil, *all* data would change (brake horsepower, Q , H , and η) due to the large change in viscosity (Reynolds number). Again this should become clear with the similarity rules.

Net Positive-Suction Head

In the top of Fig. 11.7 is plotted the *net positive-suction head* (NPSH), which is the head required at the pump inlet to keep the liquid from cavitating or boiling. The pump inlet or suction side is the low-pressure point where cavitation will first occur. The NPSH is defined as

$$\text{NPSH} = \frac{p_i}{\rho g} + \frac{V_i^2}{2g} - \frac{p_v}{\rho g} \quad (11.19)$$

where p_i and V_i are the pressure and velocity at the pump inlet and p_v is the vapor pressure of the liquid. Given the left-hand side, NPSH, from the pump performance curve, we must ensure that the right-hand side is equal or greater in the actual system to avoid cavitation.

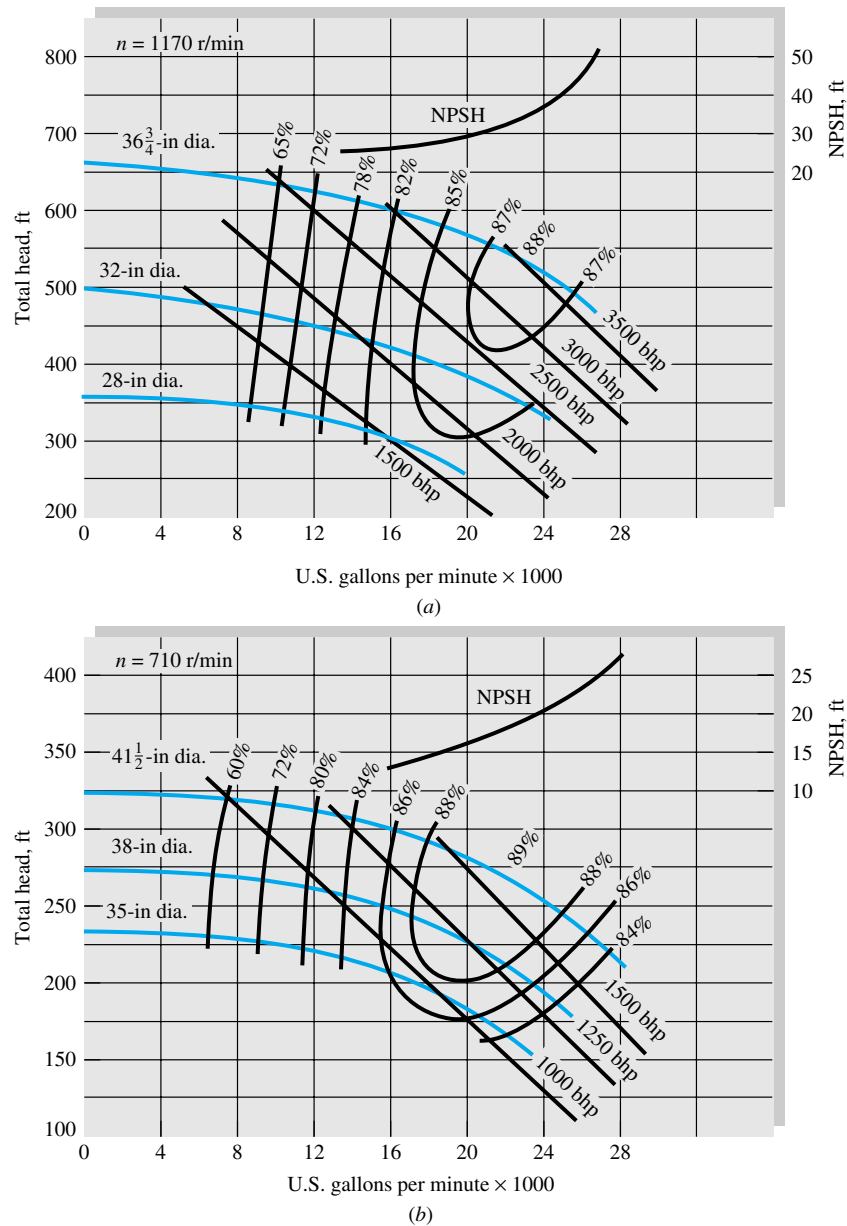


Fig. 11.7 Measured-performance curves for two models of a centrifugal water pump: (a) basic casing with three impeller sizes; (b) 20 percent larger casing with three larger impellers at slower speed. (Courtesy of Ingersoll-Rand Corporation, Cameron Pump Division.)

If the pump inlet is placed at a height Z_i above a reservoir whose free surface is at pressure p_a , we can use Bernoulli's equation to rewrite NPSH as

$$\text{NPSH} = \frac{p_a}{\rho g} - Z_i - h_{fi} - \frac{p_v}{\rho g} \quad (11.20)$$

where h_{fi} is the friction-head loss between the reservoir and the pump inlet. Knowing p_a and h_{fi} , we can set the pump at a height Z_i which will keep the right-hand side greater than the "required" NPSH plotted in Fig. 11.7.

If cavitation does occur, there will be pump noise and vibration, pitting damage to the impeller, and a sharp dropoff in pump head and discharge. In some liquids this deterioration starts before actual boiling, as dissolved gases and light hydrocarbons are liberated.

Deviations from Ideal Pump Theory

The actual pump head data in Fig. 11.7 differ considerably from ideal theory, Eq. (11.18). Take, e.g., the 36.75-in-diameter pump at 1170 r/min in Fig. 11.7a. The theoretical shutoff head is

$$H_0(\text{ideal}) = \frac{\omega^2 r_2^2}{g} = \frac{[1170(2\pi/60) \text{ rad/s}]^2 [(36.75/2)/(12) \text{ ft}]^2}{32.2 \text{ ft/s}^2} = 1093 \text{ ft}$$

From Fig. 11.7a, at $Q = 0$, we read the actual shutoff head to be only 670 ft, or 61 percent of the theoretical value. This is a sharp dropoff and is indicative of nonrecoverable losses of three types:

1. *Impeller recirculation loss*, significant only at low flow rates
2. *Friction losses* on the blade and passage surfaces, which increase monotonically with the flow rate
3. “*Shock*” loss due to mismatch between the blade angles and the inlet flow direction, especially significant at high flow rates

These are complicated three-dimensional-flow effects and hence are difficult to predict. Although, as mentioned, numerical (CFD) techniques are becoming more important [42], modern performance prediction is still a blend of experience, empirical correlations, idealized theory, and CFD modifications [45].

EXAMPLE 11.2

The 32-in pump of Fig. 11.7a is to pump 24,000 gal/min of water at 1170 r/min from a reservoir whose surface is at 14.7 lbf/in² absolute. If head loss from reservoir to pump inlet is 6 ft, where should the pump inlet be placed to avoid cavitation for water at (a) 60°F, $p_v = 0.26$ lbf/in² absolute, SG = 1.0 and (b) 200°F, $p_v = 11.52$ lbf/in² absolute, SG = 0.9635?

Solution

Part (a) For either case read from Fig. 11.7a at 24,000 gal/min that the required NPSH is 40 ft. For this case $\rho g = 62.4$ lbf/ft³. From Eq. (11.20) it is necessary that

$$\text{NPSH} \leq \frac{p_a - p_v}{\rho g} - Z_i - h_{fi}$$

or
$$40 \text{ ft} \leq \frac{(14.7 - 0.26)(144)}{62.4} - Z_i - 6.0$$

or
$$Z_i \leq 27.3 - 40 = -12.7 \text{ ft} \quad \text{Ans. (a)}$$

The pump must be placed at least 12.7 ft *below* the reservoir surface to avoid cavitation.

Part (b) For this case $\rho g = 62.4(0.9635) = 60.1$ lbf/ft³. Equation (11.20) applies again with the higher p_v

$$40 \text{ ft} \leq \frac{(14.7 - 11.52)(144)}{60.1} - Z_i - 6.0$$

$$\text{or} \quad Z_i \leq 1.6 - 40 = -38.4 \text{ ft} \quad \text{Ans. (b)}$$

The pump must now be placed at least 38.4 ft below the reservoir surface. These are unusually stringent conditions because a large, high-discharge pump requires a large NPSH.

Dimensionless Pump Performance

For a given pump design, the output variables H and brake horsepower should be dependent upon discharge Q , impeller diameter D , and shaft speed n , at least. Other possible parameters are the fluid density ρ , viscosity μ , and surface roughness ϵ . Thus the performance curves in Fig. 11.7 are equivalent to the following assumed functional relations:²

$$gH = f_1(Q, D, n, \rho, \mu, \epsilon) \quad \text{bhp} = f_2(Q, D, n, \rho, \mu, \epsilon) \quad (11.21)$$

This is a straightforward application of dimensional-analysis principles from Chap. 5. As a matter of fact, it was given as an exercise (Prob. 5.20). For each function in Eq. (11.21) there are seven variables and three primary dimensions (M , L , and T); hence we expect $7 - 3 = 4$ dimensionless pi's, and that is what we get. You can verify as an exercise that appropriate dimensionless forms for Eqs. (11.21) are

$$\begin{aligned} \frac{gH}{n^2 D^2} &= g_1 \left(\frac{Q}{nD^3}, \frac{\rho n D^2}{\mu}, \frac{\epsilon}{D} \right) \\ \frac{\text{bhp}}{\rho n^3 D^5} &= g_2 \left(\frac{Q}{nD^3}, \frac{\rho n D^2}{\mu}, \frac{\epsilon}{D} \right) \end{aligned} \quad (11.22)$$

The quantities $\rho n D^2 / \mu$ and ϵ / D are recognized as the Reynolds number and roughness ratio, respectively. Three new pump parameters have arisen:

$$\begin{aligned} \text{Capacity coefficient } C_Q &= \frac{Q}{nD^3} \\ \text{Head coefficient } C_H &= \frac{gH}{n^2 D^2} \\ \text{Power coefficient } C_P &= \frac{\text{bhp}}{\rho n^3 D^5} \end{aligned} \quad (11.23)$$

Note that only the power coefficient contains fluid density, the parameters C_Q and C_H being kinematic types.

Figure 11.7 gives no warning of viscous or roughness effects. The Reynolds numbers are from 0.8 to 1.5×10^7 , or fully turbulent flow in all passages probably. The roughness is not given and varies greatly among commercial pumps. But at such high Reynolds numbers we expect more or less the same percentage effect on all these pumps. Therefore it is common to assume that the Reynolds number and the roughness ratio have a constant effect, so that Eqs. (11.23) reduce to, approximately,

$$C_H \approx C_H(C_Q) \quad C_P \approx C_P(C_Q) \quad (11.24)$$

² We adopt gH as a variable instead of H for dimensional reasons.

For geometrically similar pumps, we expect head and power coefficients to be (nearly) unique functions of the capacity coefficient. We have to watch out that the pumps are geometrically similar or nearly so because (1) manufacturers put different-sized impellers in the same casing, thus violating geometric similarity, and (2) large pumps have smaller ratios of roughness and clearances to impeller diameter than small pumps. In addition, the more viscous liquids will have significant Reynolds-number effects; e.g., a factor-of-3 or more viscosity increase causes a clearly visible effect on C_H and C_P .

The efficiency η is already dimensionless and is uniquely related to the other three. It varies with C_Q also

$$\eta \equiv \frac{C_H C_Q}{C_P} = \eta(C_Q) \quad (11.25)$$

We can test Eqs. (11.24) and (11.25) from the data of Fig. 11.7. The impeller diameters of 32 and 38 in are approximately 20 percent different in size, and so their ratio of impeller to casing size is the same. The parameters C_Q , C_H , and C_P are computed with n in r/s, Q in ft³/s (gal/min $\times 2.23 \times 10^{-3}$), H and D in ft, $g = 32.2$ ft/s², and brake horsepower in horsepower times 550 ft \cdot lbf/(s \cdot hp). The nondimensional data are then plotted in Fig. 11.8. A dimensionless suction-head coefficient is also defined

$$C_{HS} = \frac{g(\text{NPSH})}{n^2 D^2} = C_{HS}(C_Q) \quad (11.26)$$

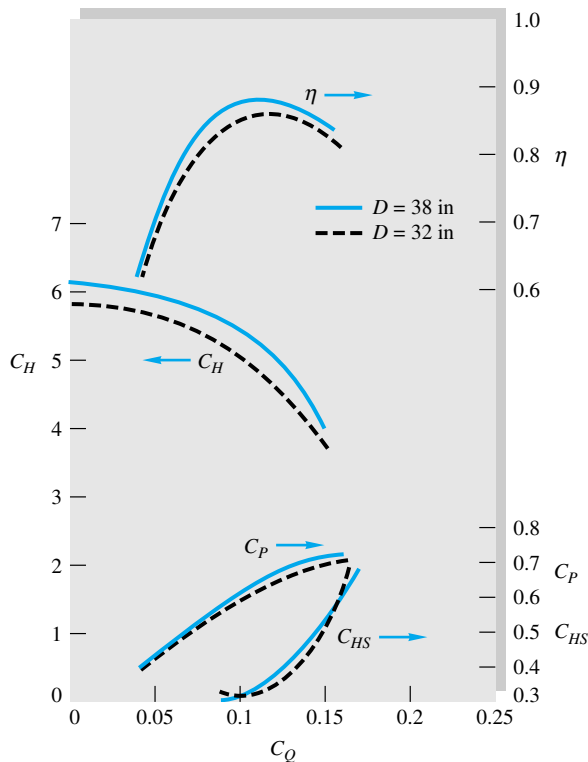


Fig. 11.8 Nondimensional plot of the pump performance data from Fig. 11.7. These numbers are not representative of other pump designs.

The coefficients C_P and C_{HS} are seen to correlate almost perfectly into a single function of C_Q , while η and C_H data deviate by a few percent. The last two parameters are more sensitive to slight discrepancies in model similarity; since the larger pump has smaller roughness and clearance ratios and a 40 percent larger Reynolds number, it develops slightly more head and is more efficient. The overall effect is a resounding victory for dimensional analysis.

The best-efficiency point in Fig. 11.8 is approximately

$$\eta_{\max} \approx 0.88: \quad \begin{aligned} C_{Q^*} &\approx 0.115 & C_{P^*} &\approx 0.65 \\ C_{H^*} &\approx 5.0 & C_{HS^*} &\approx 0.37 \end{aligned} \quad (11.27)$$

These values can be used to estimate the BEP performance of any size pump in this geometrically similar family. In like manner, the shutoff head is $C_H(0) \approx 6.0$, and by extrapolation the shutoff power is $C_P(0) \approx 0.25$ and the maximum discharge is $C_{Q,\max} \approx 0.23$. Note, however, that Fig. 11.8 gives no reliable information about, say, the 28- or 35-in impellers in Fig. 11.7, which have a different impeller-to-casing-size ratio and thus must be correlated separately.

By comparing values of n^2D^2 , nD^3 , and n^3D^5 for two pumps in Fig. 11.7 we can see readily why the large pump had the same discharge but less power and head:

	D , ft	n , r/s	Discharge nD^3 , ft ³ /s	Head n^2D^2/g , ft	Power $\rho n^3D^5/550$, hp
Fig. 11.7a	32/12	1170/60	370	84	3527
Fig. 11.7b	38/12	710/60	376	44	1861
Ratio	—	—	1.02	0.52	0.53

Discharge goes as nD^3 , which is about the same for both pumps. Head goes as n^2D^2 and power as n^3D^5 for the same ρ (water), and these are about half as much for the larger pump. The NPSH goes as n^2D^2 and is also half as much for the 38-in pump.

EXAMPLE 11.3

A pump from the family of Fig. 11.8 has $D = 21$ in and $n = 1500$ r/min. Estimate (a) discharge, (b) head, (c) pressure rise, and (d) brake horsepower of this pump for water at 60°F and best efficiency.

Solution

Part (a) In BG units take $D = 21/12 = 1.75$ ft and $n = 1500/60 = 25$ r/s. At 60°F, ρ of water is 1.94 slugs/ft³. The BEP parameters are known from Fig. 11.8 or Eqs. (11.27). The BEP discharge is thus

$$Q^* = C_{Q^*} n D^3 = 0.115(25)(1.75)^3 = (15.4 \text{ ft}^3/\text{s})(448.8) = 6900 \text{ gal/min} \quad \text{Ans. (a)}$$

Part (b) Similarly, the BEP head is

$$H^* = \frac{C_{H^*} n^2 D^2}{g} = \frac{5.0(25)^2(1.75)^2}{32.2} = 300\text{-ft water} \quad \text{Ans. (b)}$$

Part (c) Since we are not given elevation or velocity-head changes across the pump, we neglect them and estimate

$$\Delta p \approx \rho g H = 1.94(32.2)(300) = 18,600 \text{ lbf/ft}^2 = 129 \text{ lbf/in}^2 \quad \text{Ans. (c)}$$

Part (d) Finally, the BEP power is

$$\begin{aligned} P^* &= C_{P^*} \rho n^3 D^5 = 0.65(1.94)(25)^3(1.75)^5 \\ &= \frac{323,000 \text{ ft} \cdot \text{lbf/s}}{550} = 590 \text{ hp} \end{aligned} \quad \text{Ans. (d)}$$

EXAMPLE 11.4

We want to build a pump from the family of Fig. 11.8, which delivers 3000 gal/min water at 1200 r/min at best efficiency. Estimate (a) the impeller diameter, (b) the maximum discharge, (c) the shutoff head, and (d) the NPSH at best efficiency.

Solution

Part (a) 3000 gal/min = 6.68 ft³/s and 1200 r/min = 20 r/s. At BEP we have

$$Q^* = C_{Q^*} n D^3 = 6.68 \text{ ft}^3/\text{s} = (0.115)(20)D^3$$

or
$$D = \left[\frac{6.68}{0.115(20)} \right]^{1/3} = 1.43 \text{ ft} = 17.1 \text{ in} \quad \text{Ans. (a)}$$

Part (b) The maximum Q is related to Q^* by a ratio of capacity coefficients

$$Q_{\max} = \frac{Q^* C_{Q, \max}}{C_{Q^*}} \approx \frac{3000(0.23)}{0.115} = 6000 \text{ gal/min} \quad \text{Ans. (b)}$$

Part (c) From Fig. 11.8 we estimated the shutoff head coefficient to be 6.0. Thus

$$H(0) \approx \frac{C_H(0)n^2 D^2}{g} = \frac{6.0(20)^2(1.43)^2}{32.2} = 152 \text{ ft} \quad \text{Ans. (c)}$$

Part (d) Finally, from Eq. (11.27), the NPSH at BEP is approximately

$$\text{NPSH}^* = \frac{C_{HS^*} n^2 D^2}{g} = \frac{0.37(20)^2(1.43)^2}{32.2} = 9.4 \text{ ft} \quad \text{Ans. (d)}$$

Since this a small pump, it will be less efficient than the pumps in Fig. 11.8, probably about 85 percent maximum.

Similarity Rules

The success of Fig. 11.8 in correlating pump data leads to simple rules for comparing pump performance. If pump 1 and pump 2 are from the same geometric family and are operating at homologous points (the same dimensionless position on a chart such as Fig. 11.8), their flow rates, heads, and powers will be related as follows:

$$\frac{Q_2}{Q_1} = \frac{n_2}{n_1} \left(\frac{D_2}{D_1} \right)^3 \quad \frac{H_2}{H_1} = \left(\frac{n_2}{n_1} \right)^2 \left(\frac{D_2}{D_1} \right)^2$$

$$\frac{P_2}{P_1} = \frac{\rho_2}{\rho_1} \left(\frac{n_2}{n_1}\right)^3 \left(\frac{D_2}{D_1}\right)^5 \quad (11.28)$$

These are the *similarity rules*, which can be used to estimate the effect of changing the fluid, speed, or size on any dynamic turbomachine—pump or turbine—within a geometrically similar family. A graphic display of these rules is given in Fig. 11.9, showing the effect of speed and diameter changes on pump performance. In Fig. 11.9a the size is held constant and the speed is varied 20 percent, while Fig. 11.9b shows a 20 percent size change at constant speed. The curves are plotted to scale but with arbitrary units. The speed effect (Fig. 11.9a) is substantial, but the size effect (Fig. 11.9b) is even more dramatic, especially for power, which varies as D^5 . Generally we see that a given pump family can be adjusted in size and speed to fit a variety of system characteristics.

Strictly speaking, we would expect for perfect similarity that $\eta_1 = \eta_2$, but we have seen that larger pumps are more efficient, having a higher Reynolds number and lower roughness and clearance ratios. Two empirical correlations are recommended for maximum efficiency. One, developed by Moody [43] for turbines but also used for pumps, is a size effect. The other, suggested by Anderson [44] from thousands of pump tests, is a flow-rate effect:

$$\text{Size changes [43]:} \quad \frac{1 - \eta_2}{1 - \eta_1} \approx \left(\frac{D_1}{D_2}\right)^{1/4} \quad (11.29a)$$

$$\text{Flow-rate changes [44]:} \quad \frac{0.94 - \eta_2}{0.94 - \eta_1} \approx \left(\frac{Q_1}{Q_2}\right)^{0.32} \quad (11.29b)$$

Anderson's formula (11.29b) makes the practical observation that even an infinitely large pump will have losses. He thus proposes a maximum possible efficiency of 94 percent, rather than 100 percent. Anderson recommends that the same formula be used

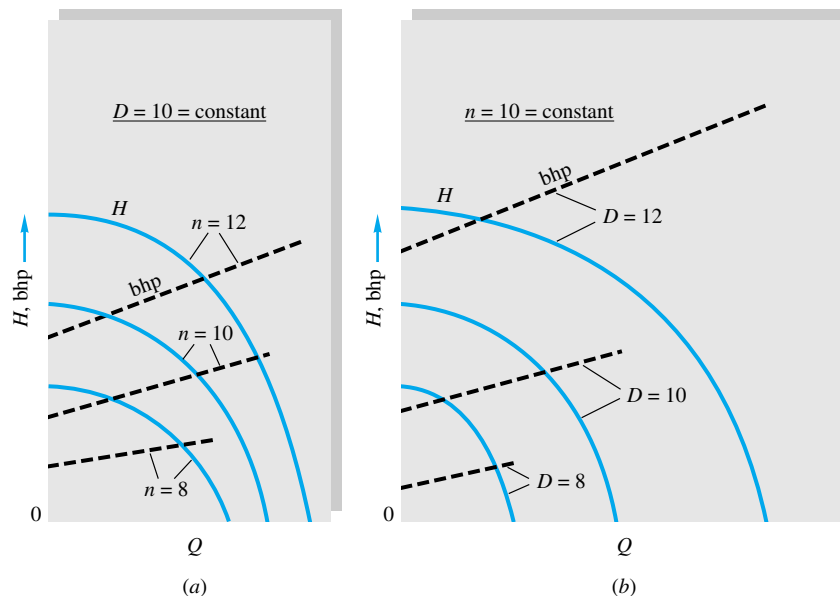


Fig. 11.9 Effect of changes in size and speed on homologous pump performance: (a) 20 percent change in speed at constant size; (b) 20 percent change in size at constant speed.

for turbines if the constant 0.94 is replaced by 0.95. The formulas in Eq. (11.29) assume the same value of surface roughness for both machines—one could micropolish a small pump and achieve the efficiency of a larger machine.

Effect of Viscosity

Centrifugal pumps are often used to pump oils and other viscous liquids up to 1000 times the viscosity of water. But the Reynolds numbers become low turbulent or even laminar, with a strong effect on performance. Figure 11.10 shows typical test curves of head and brake horsepower versus discharge. High viscosity causes a dramatic drop in head and discharge and increases in power requirements. The efficiency also drops substantially according to the following typical results:

μ/μ_{water}	1.0	10.0	100	1000
$\eta_{\text{max, \%}}$	85	76	52	11

Beyond about $300\mu_{\text{water}}$ the deterioration in performance is so great that a positive-displacement pump is recommended.

11.4 Mixed- and Axial-Flow Pumps: The Specific Speed

We have seen from the previous section that the modern centrifugal pump is a formidable device, able to deliver very high heads and reasonable flow rates with excellent efficiency. It can match many system requirements. But basically the centrifugal pump is a high-head, low-flow machine, whereas there are many applications requiring low head and high discharge. To see that the centrifugal design is not convenient for such systems, consider the following example.

EXAMPLE 11.5

We want to use a centrifugal pump from the family of Fig. 11.8 to deliver 100,000 gal/min of water at 60°F with a head of 25 ft. What should be (a) the pump size and speed and (b) brake horsepower, assuming operation at best efficiency?

Solution

Part (a) Enter the known head and discharge into the BEP parameters from Eq. (11.27):

$$H^* = 25 \text{ ft} = \frac{C_H n^2 D^2}{g} = \frac{5.0 n^2 D^2}{32.2}$$

$$Q^* = 100,000 \text{ gal/min} = 222.8 \text{ ft}^3/\text{s} = C_Q n D^3 = 0.115 n D^3$$

The two unknowns are n and D . Solve simultaneously for

$$D = 12.4 \text{ ft} \quad n = 1.03 \text{ r/s} = 62 \text{ r/min} \quad \text{Ans. (a)}$$



If you wish to avoid algebraic manipulation, simply program the above two simultaneous equations in EES, using English units:

$$25 = 5.0 * n^2 * D^2 / 32.2$$

$$222.8 = 0.115 * n * D^3$$

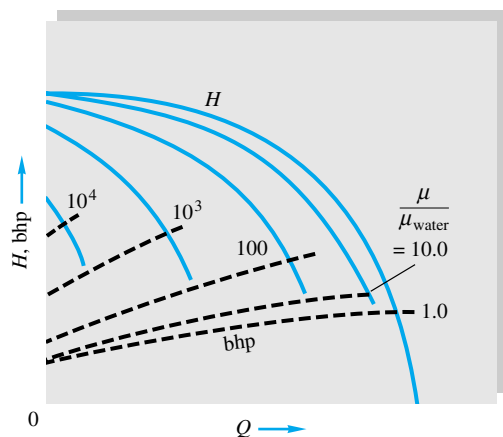


Fig. 11.10 Effect of viscosity on centrifugal pump performance.

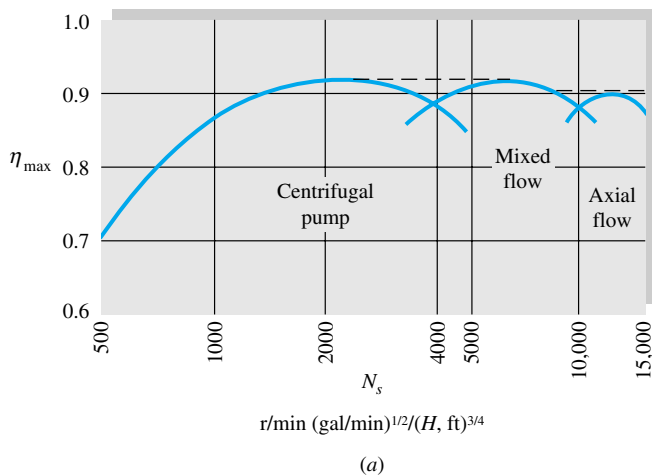
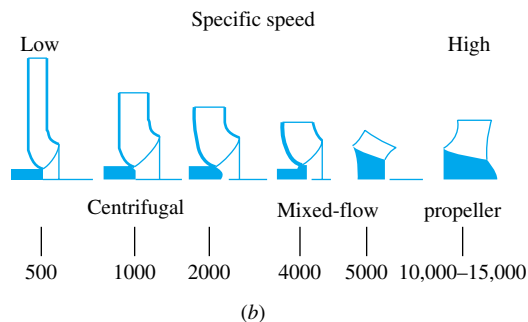


Fig. 11.11 (a) Optimum efficiency and (b) vane design of dynamic-pump families as a function of specific speed.



Specify in Variable Information that n and D are positive, and EES promptly returns the correct solution: $D = 12.36$ ft and $n = 1.027$ r/s.

Part (b) The most efficient horsepower is then, from Eq. (11.27),

$$\text{bhp}^* \approx C_{p^*} \rho n^3 D^5 = \frac{0.65(1.94)(1.03)^3(12.4)^5}{550} = 720 \text{ hp} \quad \text{Ans. (b)}$$

The solution to Example 11.5 is mathematically correct but results in a grotesque pump: an impeller more than 12 ft in diameter, rotating so slowly one can visualize oxen walking in a circle turning the shaft.

There are other dynamic-pump designs which do provide low head and high discharge. For example, there is a type of 38-in, 710 r/min pump, e.g., with the same input parameters as Fig. 11.7b, which will deliver the 25-ft head and 100,000 gal/min flow rate called for in Example 11.5. This is done by allowing the flow to pass through the impeller with an axial-flow component and less centrifugal component. The passages can be opened up to the increased flow rate with very little size increase, but the drop in radial outlet velocity decreases the head produced. These are the mixed-flow (part radial, part axial) and axial-flow (propeller-type) families of dynamic pump. Some vane designs are sketched in Fig. 11.11, which introduces an interesting new “design” parameter, the specific speed N_s or N'_s .

The Specific Speed

Most pump applications involve a known head and discharge for the particular system, plus a speed range dictated by electric motor speeds or cavitation requirements. The designer then selects the best size and shape (centrifugal, mixed, axial) for the pump. To help this selection, we need a dimensionless parameter involving speed, discharge, and head but not size. This is accomplished by eliminating the diameter between C_Q and C_H , applying the result only to the BEP. This ratio is called the *specific speed* and has both a dimensionless form and a somewhat lazy, practical form:

$$\text{Rigorous form:} \quad N'_s = \frac{C_{Q^*}^{1/2}}{C_{H^*}^{3/4}} = \frac{n(Q^*)^{1/2}}{(gH^*)^{3/4}} \quad (11.30a)$$

$$\text{Lazy but common:} \quad N_s = \frac{(\text{r/min})(\text{gal/min})^{1/2}}{[H(\text{ft})]^{3/4}} \quad (11.30b)$$

In other words, practicing engineers do not bother to change n to revolutions per second or Q^* to cubic feet per second or to include gravity with head, although the latter would be necessary for, say, a pump on the moon. The conversion factor is

$$N_s = 17,182N'_s$$

Note that N_s is applied only to BEP; thus a single number characterizes an entire family of pumps. For example, the family of Fig. 11.8 has $N'_s \approx (0.115)^{1/2}/(5.0)^{3/4} = 0.1014$, $N_s = 1740$, regardless of size or speed.

It turns out that the specific speed is directly related to the most efficient pump design, as shown in Fig. 11.11. Low N_s means low Q and high H , hence a centrifugal pump, and large N_s implies an axial pump. The centrifugal pump is best for N_s between 500 and 4000, the mixed-flow pump for N_s between 4000 and 10,000, and the axial-flow pump for N_s above 10,000. Note the changes in impeller shape as N_s increases.

Suction Specific Speed

If we use NPSH rather than H in Eq. (11.30), the result is called *suction specific speed*

$$\text{Rigorous:} \quad N'_{ss} = \frac{nQ^{1/2}}{(g \text{NPSH})^{3/4}} \quad (11.31a)$$

$$\text{Lazy:} \quad N_{ss} = \frac{(\text{r/min})(\text{gal/min})^{1/2}}{[\text{NPSH}(\text{ft})]^{3/4}} \quad (11.31b)$$

where NPSH denotes the available suction head of the system. Data from Wislicenus [4] show that a given pump is in danger of inlet cavitation if

$$N'_{ss} \geq 0.47 \quad N_{ss} \geq 8100$$

In the absence of test data, this relation can be used, given n and Q , to estimate the minimum required NPSH.

Axial-Flow Pump Theory

A multistage axial-flow geometry is shown in Fig. 11.12a. The fluid essentially passes almost axially through alternate rows of fixed *stator* blades and moving *rotor* blades. The incompressible-flow assumption is frequently used even for gases, because the pressure rise per stage is usually small.

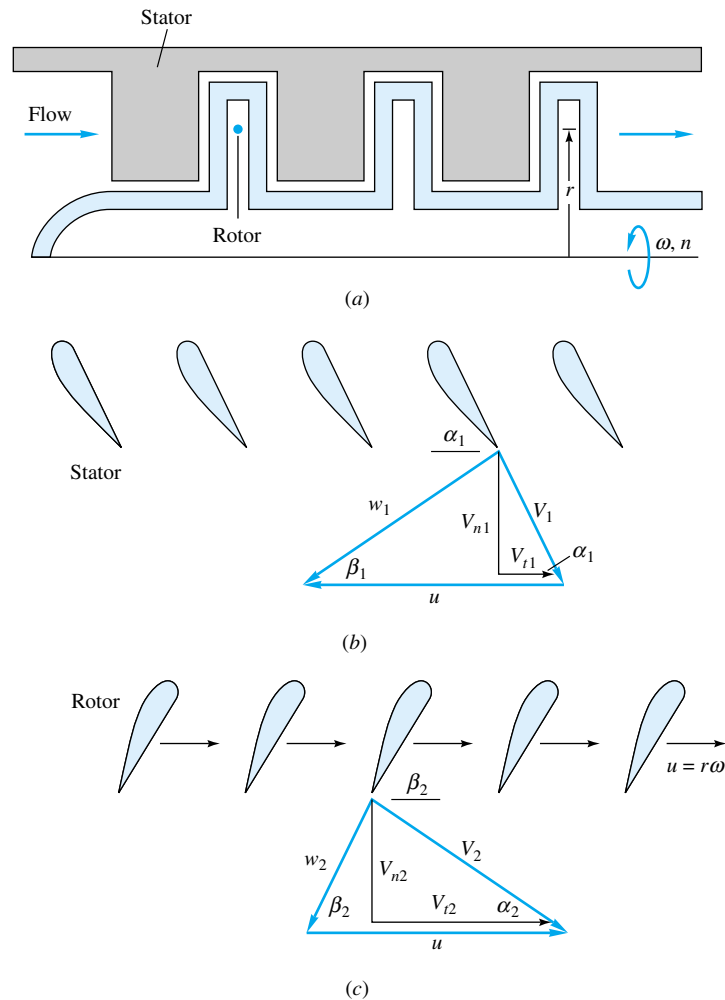


Fig. 11.12 Analysis of an axial-flow pump: (a) basic geometry; (b) stator blades and exit-velocity diagram; (c) rotor blades and exit-velocity diagram.

The simplified vector-diagram analysis assumes that the flow is one-dimensional and leaves each blade row at a relative velocity exactly parallel to the exit blade angle. Figure 11.12b shows the stator blades and their exit-velocity diagram. Since the stator is fixed, ideally the absolute velocity V_1 is parallel to the trailing edge of the blade. After vectorially subtracting the rotor tangential velocity u from V_1 , we obtain the velocity w_1 relative to the rotor, which ideally should be parallel to the rotor leading edge.

Figure 11.12c shows the rotor blades and their exit-velocity diagram. Here the relative velocity w_2 is parallel to the blade trailing edge, while the absolute velocity V_2 should be designed to enter smoothly the next row of stator blades.

The theoretical power and head are given by Euler's turbine relation (11.11). Since there is no radial flow, the inlet and exit rotor speeds are equal, $u_1 = u_2$, and one-dimensional continuity requires that the axial-velocity component remain constant

$$V_{n1} = V_{n2} = V_n = \frac{Q}{A} = \text{const}$$

From the geometry of the velocity diagrams, the normal velocity (or volume flow) can be directly related to the blade rotational speed u :

$$u = \omega r_{av} = V_{n1}(\tan \alpha_1 + \tan \beta_1) = V_{n2}(\tan \alpha_2 + \tan \beta_2) \quad (11.32)$$

Thus the flow rate can be predicted from the rotational speed and the blade angles. Meanwhile, since $V_{t1} = V_{n1} \cot \alpha_1$ and $V_{t2} = u - V_{n2} \cot \beta_2$, Euler's relation (11.11) for the pump head becomes

$$\begin{aligned} gH &= uV_n(\cot \alpha_2 - \cot \alpha_1) \\ &= u^2 - uV_n(\cot \alpha_1 + \cot \beta_2) \end{aligned} \quad (11.33)$$

the preferred form because it relates to the blade angles α_1 and β_2 . The shutoff or no-flow head is seen to be $H_0 = u^2/g$, just as in Eq. (11.18) for a centrifugal pump. The blade-angle parameter $\cot \alpha_1 + \cot \beta_2$ can be designed to be negative, zero, or positive, corresponding to a rising, flat, or falling head curve, as in Fig. 11.5.

Strictly speaking, Eq. (11.33) applies only to a single streamtube of radius r , but it is a good approximation for very short blades if r denotes the average radius. For long blades it is customary to sum Eq. (11.33) in radial strips over the blade area. Such complexity may not be warranted since theory, being idealized, neglects losses and usually predicts the head and power larger than those in actual pump performance.

Performance of an Axial-Flow Pump

At high specific speeds, the most efficient choice is an axial-flow, or propeller, pump, which develops high flow rate and low head. A typical dimensionless chart for a propeller pump is shown in Fig. 11.13. Note, as expected, the higher C_Q and lower C_H compared with Fig. 11.8. The head curve drops sharply with discharge, so that a large system-head change will cause a mild flow change. The power curve drops with head also, which means a possible overloading condition if the system discharge should sud-

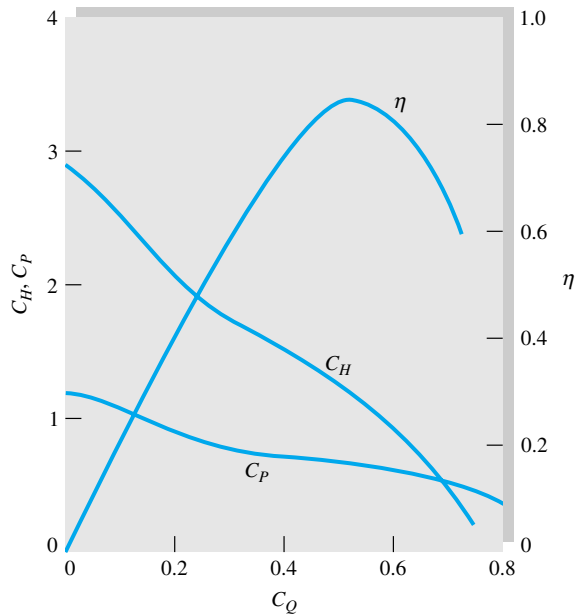


Fig. 11.13 Dimensionless performance curves for a typical axial-flow pump, $N_s = 12,000$. Constructed from data given by Stepanoff [8] for a 14-in pump at 690 r/min.

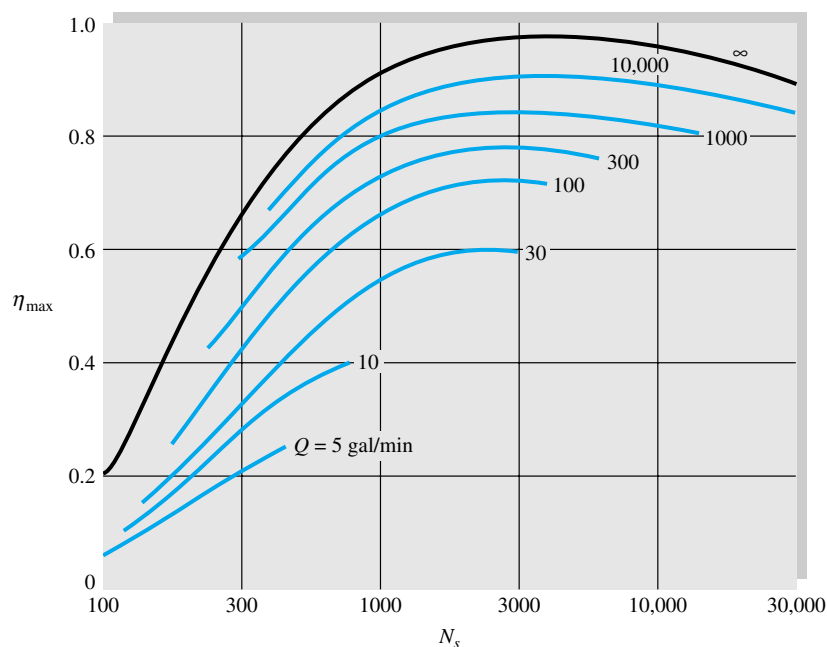


Fig. 11.14 Optimum efficiency of pumps versus capacity and specific speed. (Adapted from Refs. 4 and 31.)

denly decrease. Finally, the efficiency curve is rather narrow and triangular, as opposed to the broad, parabolic-shaped centrifugal pump efficiency (Fig. 11.8).

By inspection of Fig. 11.13, $C_{Q^*} \approx 0.55$, $C_{H^*} \approx 1.07$, $C_{P^*} \approx 0.70$, and $\eta_{\max} \approx 0.84$. From this we compute $N'_s \approx (0.55)^{1/2}/(1.07)^{3/4} = 0.705$, $N_s = 12,000$. The relatively low efficiency is due to small pump size: $d = 14$ in, $n = 690$ r/min, $Q^* = 4400$ gal/min.

A repetition of Example 11.5 using Fig. 11.13 would show that this propeller pump family can provide a 25-ft head and 100,000 gal/min discharge if $D = 46$ in and $n = 430$ r/min, with bhp = 750; this is a much more reasonable design solution, with improvements still possible at larger- N_s conditions.

Pump Performance versus Specific Speed

Specific speed is such an effective parameter that it is used as an indicator of both performance and efficiency. Figure 11.14 shows a correlation of the optimum efficiency of a pump as a function of the specific speed and capacity. Because the dimensional parameter Q is a rough measure of both size and Reynolds number, η increases with Q . When this type of correlation was first published by Wislicenus [4] in 1947, it became known as *the pump curve*, a challenge to all manufacturers. We can check that the pumps of Figs. 11.7 and 11.13 fit the correlation very well.

Figure 11.15 shows the effect of specific speed on the shape of the pump performance curves, normalized with respect to the BEP point. The numerical values shown are representative but somewhat qualitative. The high-specific-speed pumps ($N_s \approx 10,000$) have head and power curves which drop sharply with discharge, implying overload or start-up problems at low flow. Their efficiency curve is very narrow.

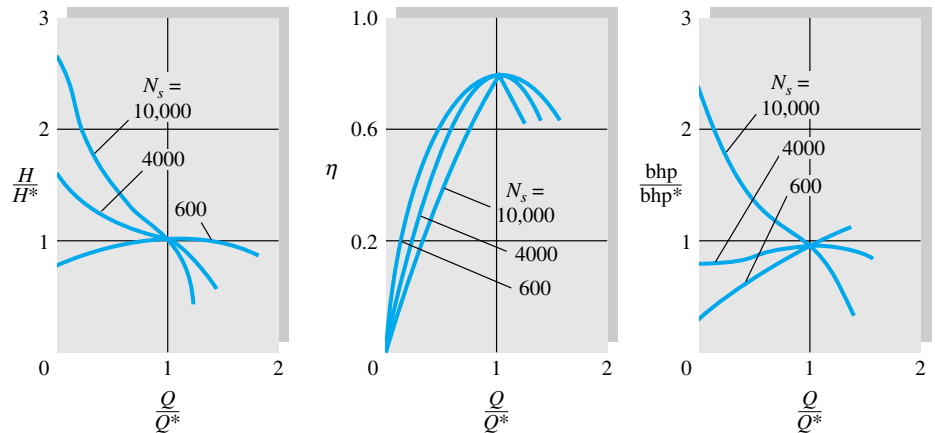


Fig. 11.15 Effect of specific speed on pump performance curves.

A low-specific-speed pump ($N_s = 600$) has a broad efficiency curve, a rising power curve, and a head curve which “droops” at shutoff, implying possible surge or hunting problems.

Computational Fluid Dynamics

The design of turbomachinery has traditionally been highly experimental, with simple theories, such as in Sec. 11.2, only able to predict trends. Dimensionless correlations, such as Fig. 11.15, are useful but require extensive experimentation. Consider that flow in a pump is three-dimensional; unsteady (both periodic and turbulent); and involves flow separation, recirculation in the impeller, unsteady blade wakes passing through the diffuser, and blade roots, tips, and clearances. It is no wonder that one-dimensional theory cannot give firm quantitative predictions.

Modern computer analysis can give realistic results and is becoming a useful tool for turbomachinery designers. A good example is Ref. 56, reporting combined experimental and computational results for a centrifugal pump diffuser. A photograph of the device is shown in Fig. 11.16a. It is made of clear Perspex, so that laser measurements of particle tracking velocimetry (LPTV) and doppler anemometry (LDA) could be taken throughout the system. The data were compared with a CFD simulation of the impeller and diffuser, using the grids shown in Fig. 11.16b. The computations used a turbulence formulation called the $k-\epsilon$ model, popular in commercial CFD codes (see Sec. 8.9). Results were good but not excellent. The CFD model predicted velocity and pressure data adequately up until flow separation, after which it was only qualitative. Clearly, CFD is developing a significant role in turbomachinery design.

11.5 Matching Pumps to System Characteristics

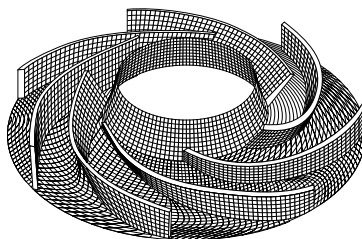
The ultimate test of a pump is its match with the operating-system characteristics. Physically, the system head must match the head produced by the pump, and this intersection should occur in the region of best efficiency.

The system head will probably contain a static-elevation change $z_2 - z_1$ plus friction losses in pipes and fittings

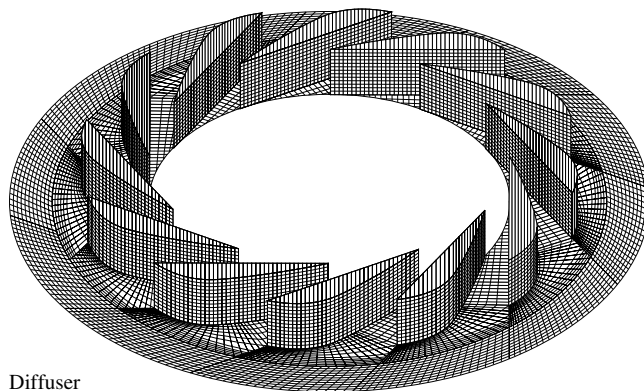
$$H_{\text{sys}} = (z_2 - z_1) + \frac{V^2}{2g} \left(\sum \frac{fL}{D} + \sum K \right) \quad (11.34)$$



(a)



Impeller



Diffuser

(b)

Fig. 11.16 Turbomachinery design now involves both experimentation and computational fluid dynamics (CFD): (a) a centrifugal impeller and diffuser (Courtesy of K. Eisele and Z. Zhang, Sulzer Innotec Ltd.); (b) a three-dimensional CFD model grid for this system. (From Ref. 56 by permission of the American Society of Mechanical Engineers.)

where ΣK denotes minor losses and V is the flow velocity in the principal pipe. Since V is proportional to the pump discharge Q , Eq. (11.34) represents a system-head curve $H_s(Q)$. Three examples are shown in Fig. 11.17: a static head $H_s = a$, static head plus laminar friction $H_s = a + bQ$, and static head plus turbulent friction $H_s = a + cQ^2$. The intersection of the system curve with the pump performance curve $H(Q)$ defines

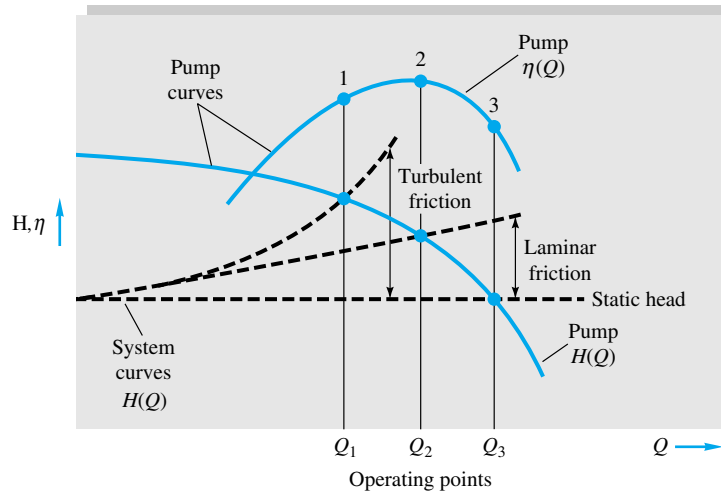


Fig. 11.17 Illustration of pump operating points for three types of system-head curves.

the operating point. In Fig. 11.17 the laminar-friction operating point is at maximum efficiency while the turbulent and static curves are off design. This may be unavoidable if system variables change, but the pump should be changed in size or speed if its operating point is consistently off design. Of course, a perfect match may not be possible because commercial pumps have only certain discrete sizes and speeds. Let us illustrate these concepts with an example.

EXAMPLE 11.6

We want to use the 32-in pump of Fig. 11.7a at 1170 r/min to pump water at 60°F from one reservoir to another 120 ft higher through 1500 ft of 16-in-ID pipe with friction factor $f = 0.030$. (a) What will the operating point and efficiency be? (b) To what speed should the pump be changed to operate at the BEP?

Solution

Part (a) For reservoirs the initial and final velocities are zero; thus the system head is

$$H_s = z_2 - z_1 + \frac{V^2}{2g} \frac{fL}{D} = 120 \text{ ft} + \frac{V^2}{2g} \frac{0.030(1500 \text{ ft})}{\frac{16}{12} \text{ ft}}$$

From continuity in the pipe, $V = Q/A = Q/[\frac{1}{4}\pi(\frac{16}{12} \text{ ft})^2]$, and so we substitute for V above to get

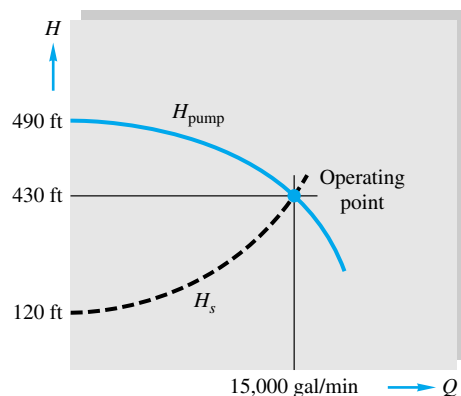
$$H_s = 120 + 0.269Q^2 \quad Q \text{ in ft}^3/\text{s} \quad (1)$$

Since Fig. 11.7a uses thousands of gallons per minute for the abscissa, we convert Q in Eq. (1) to this unit:

$$H_s = 120 + 1.335Q^2 \quad Q \text{ in } 10^3 \text{ gal/min} \quad (2)$$

We can plot Eq. (2) on Fig. 11.7a and see where it intersects the 32-in pump-head curve, as in Fig. E11.6. A graphical solution gives approximately

$$H \approx 430 \text{ ft} \quad Q \approx 15,000 \text{ gal/min}$$



E11.6

The efficiency is about 82 percent, slightly off design.

An analytic solution is possible if we fit the pump-head curve to a parabola, which is very accurate

$$H_{\text{pump}} \approx 490 - 0.26Q^2 \quad Q \text{ in } 10^3 \text{ gal/min} \quad (3)$$

Equations (2) and (3) must match at the operating point:

$$490 - 0.26Q^2 = 120 + 1.335Q^2$$

or

$$Q^2 = \frac{490 - 120}{0.26 + 1.335} = 232$$

$$Q = 15.2 \times 10^3 \text{ gal/min} = 15,200 \text{ gal/min} \quad \text{Ans. (a)}$$

$$H = 490 - 0.26(15.2)^2 = 430 \text{ ft} \quad \text{Ans. (a)}$$

Part (b) To move the operating point to BEP, we change n , which changes both $Q \propto n$ and $H \propto n^2$. From Fig. 11.7a, at BEP, $H^* \approx 386$ ft; thus for any n , $H^* = 386(n/1170)^2$. Also read $Q^* \approx 20 \times 10^3$ gal/min; thus for any n , $Q^* = 20(n/1170)$. Match H^* to the system characteristics, Eq. (2),

$$H^* = 386 \left(\frac{n}{1170} \right)^2 \approx 120 + 1.335 \left(20 \frac{n}{1170} \right)^2 \quad \text{Ans. (b)}$$

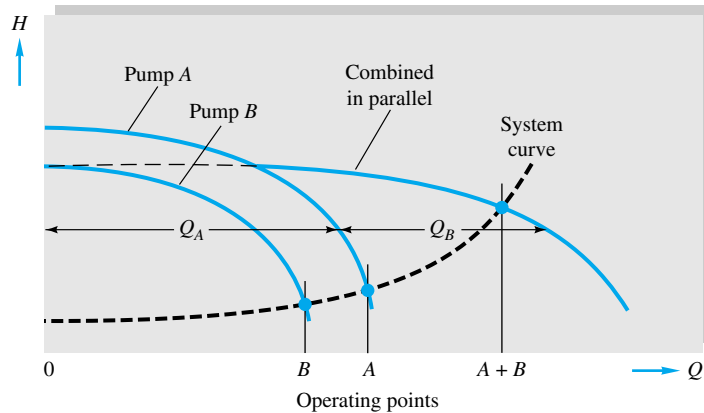
which gives $n^2 < 0$. Thus it is impossible to operate at maximum efficiency with this particular system and pump.

Pumps Combined in Parallel

If a pump provides the right head but too little discharge, a possible remedy is to combine two similar pumps in parallel, i.e., sharing the same suction and inlet conditions. A parallel arrangement is also used if delivery demand varies, so that one pump is used at low flow and the second pump is started up for higher discharges. Both pumps should have check valves to avoid backflow when one is shut down.

The two pumps in parallel need not be identical. Physically, their flow rates will sum for the same head, as illustrated in Fig. 11.18. If pump A has more head than pump B , pump B cannot be added in until the operating head is below the shutoff head of pump B . Since the system curve rises with Q , the combined delivery Q_{A+B} will be less than the separate operating discharges $Q_A + Q_B$ but certainly greater than either one.

Fig. 11.18 Performance and operating points of two pumps operating singly and combined in parallel.



For a very flat (static) curve two similar pumps in parallel will deliver nearly twice the flow. The combined brake horsepower is found by adding brake horsepower for each of pumps A and B at the same head as the operating point. The combined efficiency equals $\rho g(Q_{A+B})(H_{A+B})/(550 \text{ bhp}_{A+B})$.

If pumps A and B are not identical, as in Fig. 11.18, pump B should not be run and cannot even be started up if the operating point is above its shutoff head.

Pumps Combined in Series

If a pump provides the right discharge but too little head, consider adding a similar pump in series, with the output of pump B fed directly into the suction side of pump A. As sketched in Fig. 11.19, the physical principle for summing in series is that the two heads add at the same flow rate to give the combined-performance curve. The two

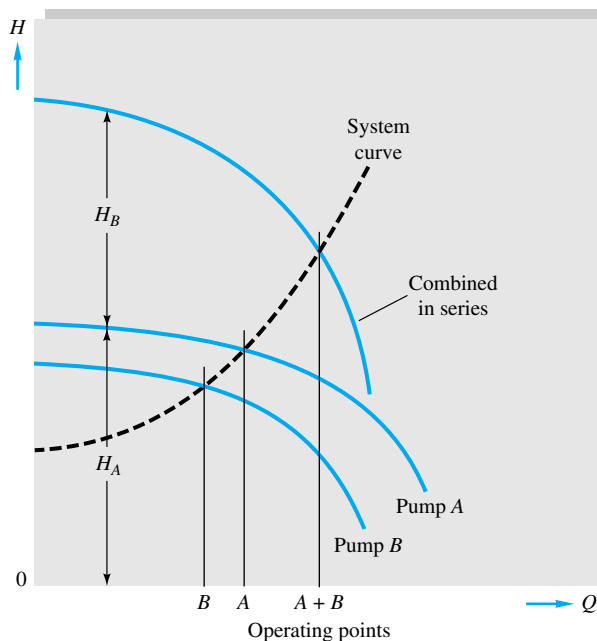


Fig. 11.19 Performance of two pumps combined in series.

need not be identical at all, since they merely handle the same discharge; they may even have different speeds, although normally both are driven by the same shaft.

The need for a series arrangement implies that the system curve is steep, i.e., requires higher head than either pump *A* or *B* can provide. The combined operating-point head will be more than either *A* or *B* separately but not as great as their sum. The combined power is the sum of brake horsepower for *A* and *B* at the operating point flow rate. The combined efficiency is

$$\frac{\rho g(Q_{A+B})(H_{A+B})}{550 \text{ bhp}_{A+B}}$$

similar to parallel pumps.

Whether pumps are used in series or in parallel, the arrangement will be uneconomical unless both pumps are operating near their best efficiency.

Multistage Pumps

For very high heads in continuous operation, the solution is a multistage pump, with the exit of one impeller feeding directly into the eye of the next. Centrifugal, mixed-flow, and axial-flow pumps have all been grouped in as many as 50 stages, with heads up to 8000 ft of water and pressure rises up to 5000 lbf/in² absolute. Figure 11.20 shows a section of a seven-stage centrifugal propane compressor which develops 300 lbf/in² rise at 40,000 ft³/min and 35,000 bhp.

Compressors

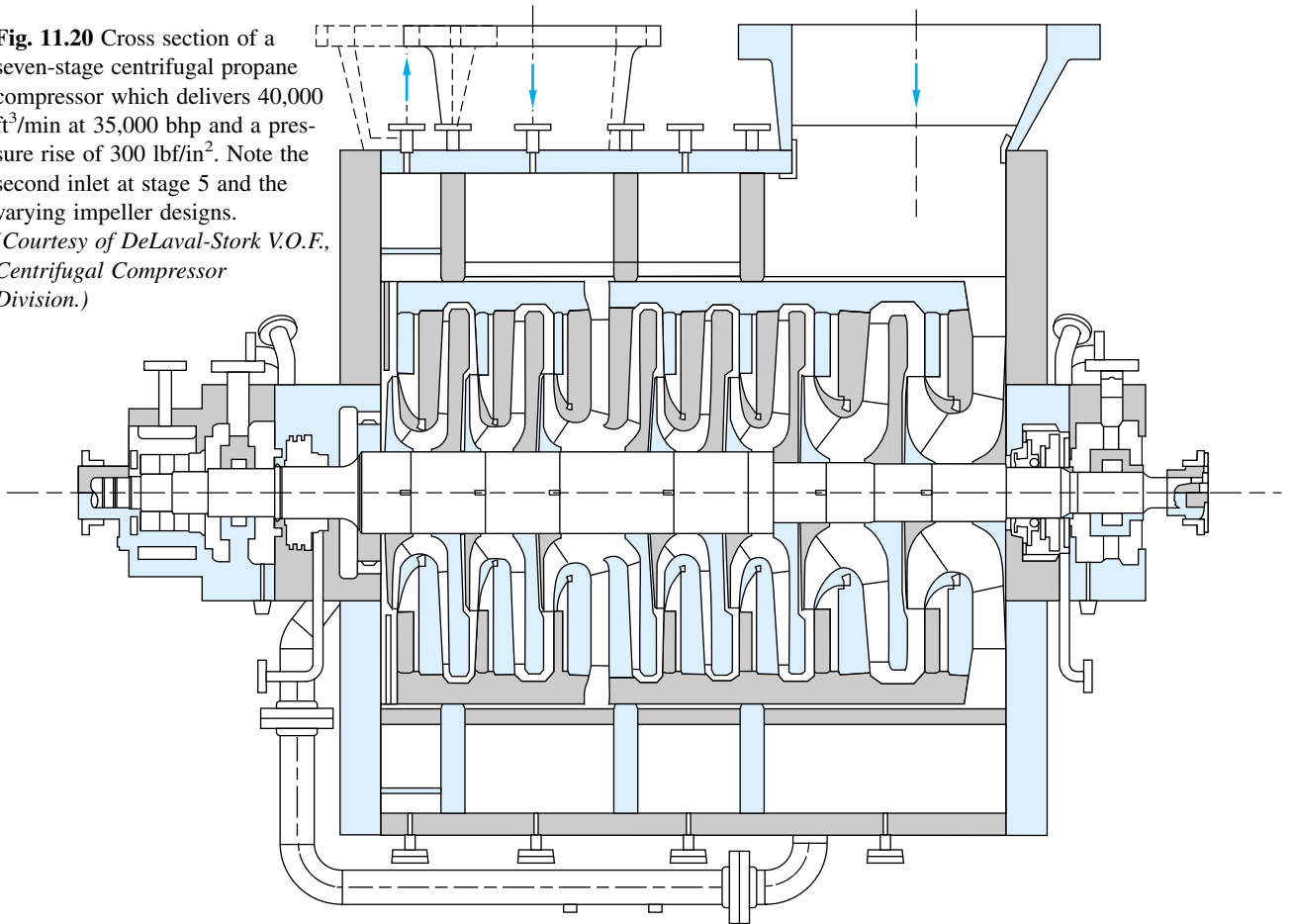
Most of the discussion in this chapter concerns incompressible flow, that is, negligible change in fluid density. Even the pump of Fig. 11.7, which can produce 600 ft of head at 1170 r/min, will only increase standard air pressure by 46 lbf/ft², about a 2 percent change in density. The picture changes at higher speeds, $\Delta p \propto n^2$, and multiple stages, where very large changes in pressure and density are achieved. Such devices are called *compressors*, as in Fig. 11.20. The concept of static head, $H = \Delta p/\rho g$, becomes inappropriate, since ρ varies. Compressor performance is measured by (1) the pressure ratio across the stage p_2/p_1 and (2) the change in stagnation enthalpy ($h_{02} - h_{01}$), where $h_0 = h + \frac{1}{2}V^2$ (see Sec. 9.3). Combining m stages in series results in $p_{\text{final}}/p_{\text{initial}} \approx (p_2/p_1)^m$. As density increases, less area is needed: note the decrease in impeller size from right to left in Fig. 11.20. Compressors may be either of the centrifugal or axial-flow type [21 to 23].

Compressor efficiency, from inlet condition 1 to final outlet f , is defined by the change in gas enthalpy, assuming an adiabatic process:

$$\eta_{\text{comp}} = \frac{h_f - h_{01}}{h_{0f} - h_{01}} \approx \frac{T_f - T_{01}}{T_{0f} - T_{01}}$$

Compressor efficiencies are similar to hydraulic machines ($\eta_{\text{max}} \approx 70$ to 80 percent), but the mass-flow range is more limited: on the low side by compressor *surge*, where blade stall and vibration occur, and on the high side by *choking* (Sec. 9.4), where the Mach number reaches 1.0 somewhere in the system. Compressor mass flow is normally plotted using the same type of dimensionless function formulated in Eq. (9.47): $\dot{m}(RT_0)^{1/2}/(D^2 p_0)$, which will reach a maximum when choking occurs. For further details, see Refs. 21 to 23.

Fig. 11.20 Cross section of a seven-stage centrifugal propane compressor which delivers 40,000 ft³/min at 35,000 bhp and a pressure rise of 300 lbf/in². Note the second inlet at stage 5 and the varying impeller designs. (Courtesy of DeLaval-Stork V.O.F., Centrifugal Compressor Division.)



EXAMPLE 11.7

Investigate extending Example 11.6 by using two 32-in pumps in parallel to deliver more flow. Is this efficient?

Solution

Since the pumps are identical, each delivers $\frac{1}{2}Q$ at the same 1170 r/min speed. The system curve is the same, and the balance-of-head relation becomes

$$H = 490 - 0.26\left(\frac{1}{2}Q\right)^2 = 120 + 1.335Q^2$$

$$\text{or} \quad Q^2 = \frac{490 - 120}{1.335 + 0.065} \quad Q = 16,300 \text{ gal/min} \quad \text{Ans.}$$

This is only 7 percent more than a single pump. Each pump delivers $\frac{1}{2}Q = 8130$ gal/min, for which the efficiency is only 60 percent. The total brake horsepower required is 3200, whereas a single pump used only 2000 bhp. This is a poor design.

EXAMPLE 11.8

Suppose the elevation change in Example 11.6 is raised from 120 to 500 ft, greater than a single 32-in pump can supply. Investigate using 32-in pumps in series at 1170 r/min.

Solution

Since the pumps are identical, the total head is twice as much and the constant 120 in the system-head curve is replaced by 500. The balance of heads becomes

$$H = 2(490 - 0.26Q^2) = 500 + 1.335Q^2$$

$$\text{or} \quad Q^2 = \frac{980 - 500}{1.335 + 0.52} \quad Q = 16.1 \times 10^3 \text{ gal/min} \quad \text{Ans.}$$

The operating head is $500 + 1.335(16.1)^2 = 845$ ft, or 97 percent more than that for a single pump in Example 11.5. Each pump is operating at 16.1×10^3 gal/min, which from Fig. 11.7a is 83 percent efficient, a pretty good match to the system. To pump at this operating point requires 4100 bhp, or about 2050 bhp for each pump.

11.6 Turbines

A turbine extracts energy from a fluid which possesses high head, but it is fatuous to say a turbine is a pump run backward. Basically there are two types, reaction and impulse, the difference lying in the manner of head conversion. In the reaction turbine, the fluid fills the blade passages, and the head change or pressure drop occurs within the impeller. Reaction designs are of the radial-flow, mixed-flow, and axial-flow types and are essentially dynamic devices designed to admit the high-energy fluid and extract its momentum. An impulse turbine first converts the high head through a nozzle into a high-velocity jet, which then strikes the blades at one position as they pass by. The impeller passages are not fluid-filled, and the jet flow past the blades is essentially at constant pressure. Reaction turbines are smaller because fluid fills all the blades at one time.

Reaction Turbines

Reaction turbines are low-head, high-flow devices. The flow is opposite that in a pump, entering at the larger-diameter section and discharging through the eye after giving up most of its energy to the impeller. Early designs were very inefficient because they lacked stationary guide vanes at the entrance to direct the flow smoothly into the impeller passages. The first efficient inward-flow turbine was built in 1849 by James B. Francis, a U.S. engineer, and all radial- or mixed-flow designs are now called *Francis turbines*. At still lower heads, a turbine can be designed more compactly with purely axial flow and is termed a *propeller turbine*. The propeller may be either fixed-blade or adjustable (Kaplan type), the latter being complicated mechanically but much more efficient at low-power settings. Figure 11.21 shows sketches of runner designs for Francis radial, Francis mixed-flow, and propeller-type turbines.

Idealized Radial Turbine Theory

The Euler turbomachine formulas (11.11) also apply to energy-extracting machines if we reverse the flow direction and reshape the blades. Figure 11.22 shows a radial turbine runner. Again assume one-dimensional frictionless flow through the blades. Adjustable inlet guide vanes are absolutely necessary for good efficiency. They bring the inlet flow to the blades at angle α_2 and absolute velocity V_2 for minimum “shock” or

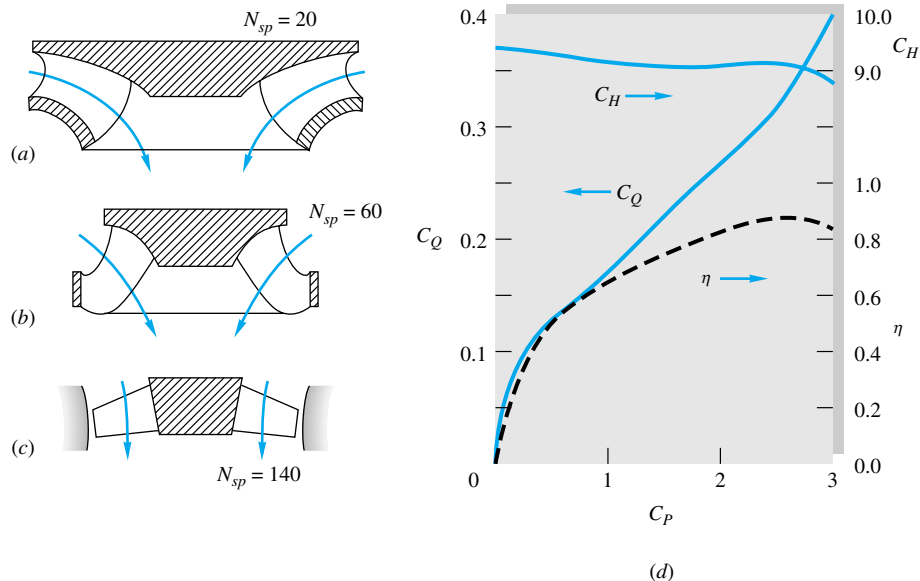


Fig. 11.21 Reaction turbines: (a) Francis, radial type; (b) Francis mixed-flow; (c) propeller axial-flow; (d) performance curves for a Francis turbine, $n = 600$ r/min, $D = 2.25$ ft, $N_{sp} = 29$.

directional-mismatch loss. After vectorially adding in the runner tip speed $u_2 = \omega r_2$, the outer blade angle should be set at angle β_2 to accommodate the relative velocity w_2 , as shown in the figure. (See Fig. 11.4 for the analogous radial-pump velocity diagrams.)

Application of the angular-momentum control-volume theorem, Eq. (3.55), to Fig. 11.22 (see Example 3.14 for a similar case) yields an idealized formula for the power P extracted by the runner:

$$P = \omega T = \rho \omega Q (r_2 V_{r2} - r_1 V_{r1}) = \rho Q (u_2 V_2 \cos \alpha_2 - u_1 V_1 \cos \alpha_1) \quad (11.35)$$

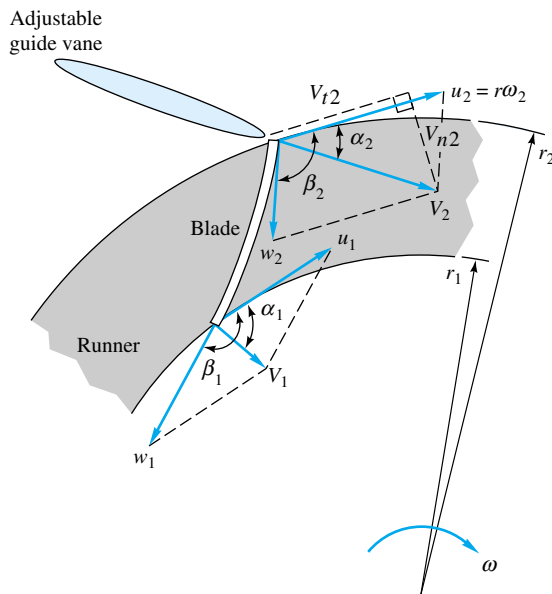


Fig. 11.22 Inlet- and outlet-velocity diagrams for an idealized radial-flow reaction turbine runner.

where V_{t2} and V_{t1} are the absolute inlet and outlet circumferential velocity components of the flow. Note that Eq. (11.35) is identical to Eq. (11.11) for a radial pump, except that the blade shapes are different.

The absolute inlet normal velocity $V_{n2} = V_2 \sin \alpha_2$ is proportional to the flow rate Q . If the flow rate changes and the runner speed u_2 is constant, the vanes must be adjusted to a new angle α_2 so that w_2 still follows the blade surface. Thus adjustable inlet vanes are very important to avoid shock loss.

Power Specific Speed

Turbine parameters are similar to those of a pump, but the dependent variable is the output brake horsepower, which depends upon the inlet flow rate Q , available head H , impeller speed n , and diameter D . The efficiency is the output brake horsepower divided by the available water horsepower $\rho g Q H$. The dimensionless forms are C_Q , C_H , and C_P , defined just as for a pump, Eqs. (11.23). If we neglect Reynolds-number and roughness effects, the functional relationships are written with C_P as the independent variable:

$$C_H = C_H(C_P) \quad C_Q = C_Q(C_P) \quad \eta = \frac{\text{bhp}}{\rho g Q H} = \eta(C_P) \quad (11.36)$$

Figure 11.21d shows typical performance curves for a small Francis radial turbine. The maximum efficiency point is called the *normal power*, and the values for this particular turbine are

$$\eta_{\max} = 0.89 \quad C_{P*} = 2.70 \quad C_{Q*} = 0.34 \quad C_{H*} = 9.03$$

A parameter which compares the output power with the available head, independent of size, is found by eliminating the diameter between C_H and C_P . It is called the *power specific speed*:

$$\text{Rigorous form:} \quad N'_{sp} = \frac{C_P^{*1/2}}{C_H^{*5/4}} = \frac{n(\text{bhp})^{1/2}}{\rho^{1/2}(gH)^{5/4}} \quad (11.37a)$$

$$\text{Lazy but common:} \quad N_{sp} = \frac{(r/\text{min})(\text{bhp})^{1/2}}{[H(\text{ft})]^{5/4}} \quad (11.37b)$$

For water, $\rho = 1.94$ slugs/ft³ and $N_{sp} = 273.3N'_{sp}$. The various turbine designs divide up nicely according to the range of power specific speed, as follows:

Turbine type	N_{sp} range	C_H range
Impulse	1–10	15–50
Francis	10–110	5–25
Propeller:		
Water	100–250	1–4
Gas, steam	25–300	10–80

Note that N_{sp} , like N_s for pumps, is defined only with respect to the BEP and has a single value for a given turbine family. In Fig. 11.21d, $N_{sp} = 273.3(2.70)^{1/2}/(9.03)^{5/4} = 29$, regardless of size.

Like pumps, turbines of large size are generally more efficient, and Eqs. (11.29) can be used as an estimate when data are lacking.

The design of a complete large-scale power-generating turbine system is a major engineering project, involving inlet and outlet ducts, trash racks, guide vanes, wicket gates, spiral cases, generator with cooling coils, bearings and transmission gears, runner blades, draft tubes, and automatic controls. Some typical large-scale reaction turbine designs are shown in Fig. 11.23. The reversible pump-and-turbine design of Fig. 11.23*d* requires special care for adjustable guide vanes to be efficient for flow in either direction.

The largest (1000-MW) hydropower designs are awesome when viewed on a human scale, as shown in Fig. 11.24. The economic advantages of small-scale model testing are evident from this photograph of the Francis turbine units at Grand Coulee Dam.

Impulse Turbines

For high head and relatively low power, i.e., low N_{sp} , not only would a reaction turbine require too high a speed but also the high pressure in the runner would require a massive casing thickness. The impulse turbine of Fig. 11.25 is ideal for this situation. Since N_{sp} is low, n will be low and the high pressure is confined to the small nozzle, which converts the head to an atmospheric pressure jet of high velocity V_j . The jet strikes the buckets and imparts a momentum change similar to that in our control-volume analysis for a moving vane in Example 3.10 or Prob. 3.51. The buckets have an elliptical split-cup shape, as in Fig. 11.25*b*. They are named *Pelton wheels*, after Lester A. Pelton (1829–1908), who produced the first efficient design.

From Example 3.10 the force and power delivered to a Pelton wheel are theoretically

$$\begin{aligned} F &= \rho Q(V_j - u)(1 - \cos \beta) \\ P &= Fu = \rho Qu(V_j - u)(1 - \cos \beta) \end{aligned} \quad (11.38)$$

where $u = 2\pi nr$ is the bucket linear velocity and r is the *pitch radius*, or distance to the jet centerline. A bucket angle $\beta = 180^\circ$ gives maximum power but is physically impractical. In practice, $\beta \approx 165^\circ$, or $1 - \cos \beta \approx 1.966$ or only 2 percent less than maximum power.

From Eq. (11.38) the theoretical power of an impulse turbine is parabolic in bucket speed u and is maximum when $dP/du = 0$, or

$$u^* = 2\pi n^* r = \frac{1}{2}V_j \quad (11.39)$$

For a perfect nozzle, the entire available head would be converted to jet velocity $V_j = (2gH)^{1/2}$. Actually, since there are 2 to 8 percent nozzle losses, a velocity coefficient C_v is used

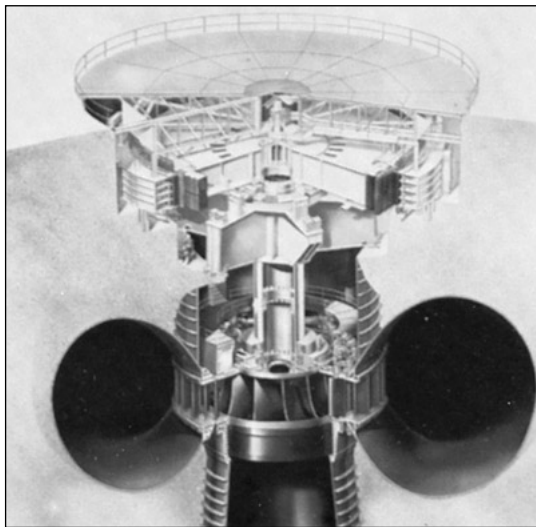
$$V_j = C_v(2gH)^{1/2} \quad 0.92 \leq C_v \leq 0.98 \quad (11.40)$$

By combining Eqs. (11.36) and (11.40), the theoretical impulse turbine efficiency becomes

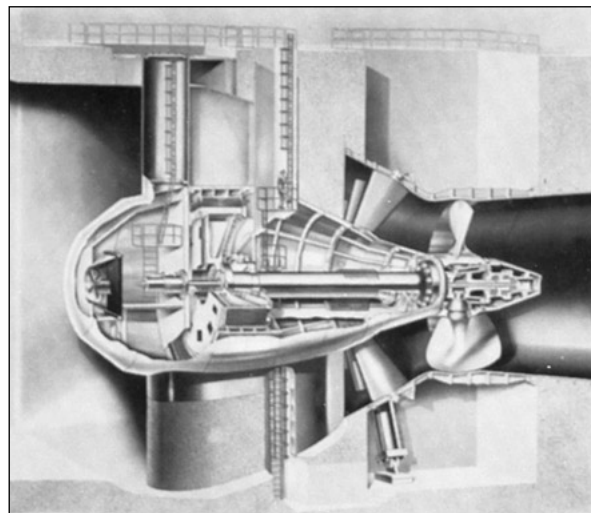
$$\eta = 2(1 - \cos \beta)\phi(C_v - \phi) \quad (11.41)$$

where $\phi = \frac{u}{(2gH)^{1/2}} =$ peripheral-velocity factor

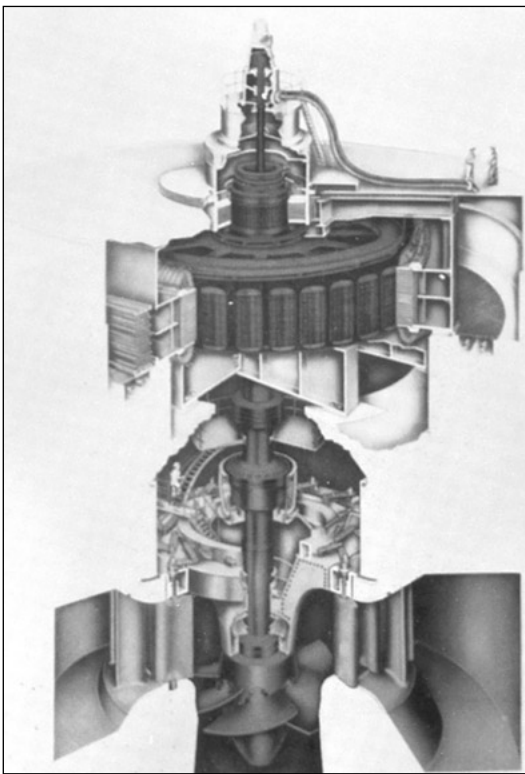
Maximum efficiency occurs at $\phi = \frac{1}{2}C_v \approx 0.47$.



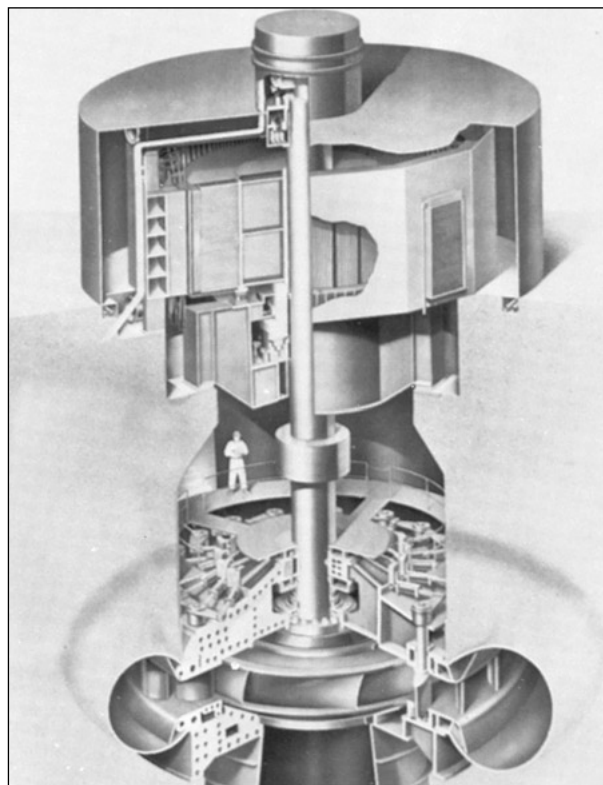
(a)



(c)



(b)



(d)

Fig. 11.23 Large-scale turbine designs depend upon available head and flow rate and operating conditions: (a) Francis (radial); (b) Kaplan (propeller); (c) bulb mounting with propeller runner; (d) reversible pump turbine with radial runner. (Courtesy of Allis-Chalmers Fluid Products Company.)

Fig. 11.24 Interior view of the 1.1-million hp (820-MW) turbine units on the Grand Coulee Dam of the Columbia River, showing the spiral case, the outer fixed vanes (“stay ring”), and the inner adjustable vanes (“wicket gates”). (Courtesy of Allis-Chalmers Fluid Products Company.)

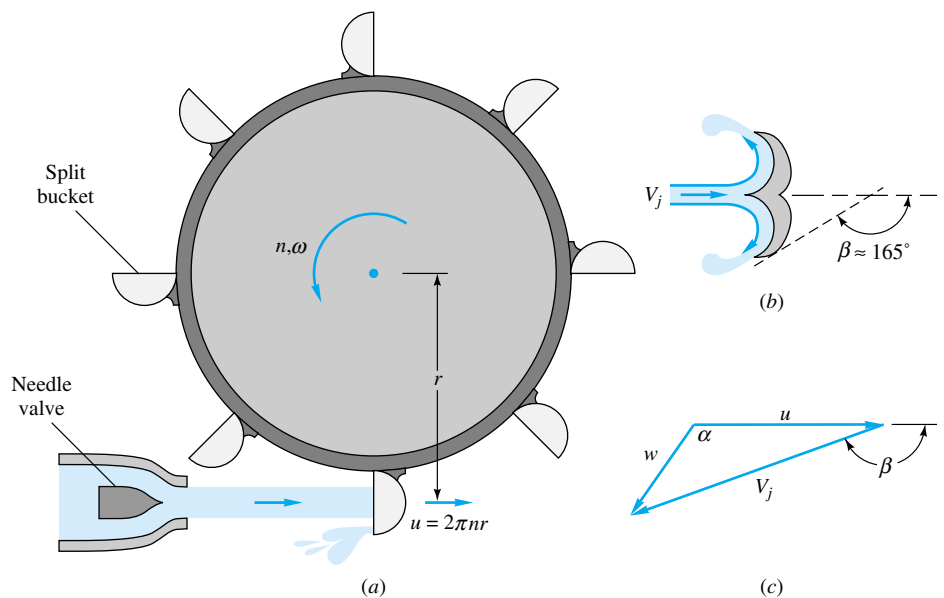
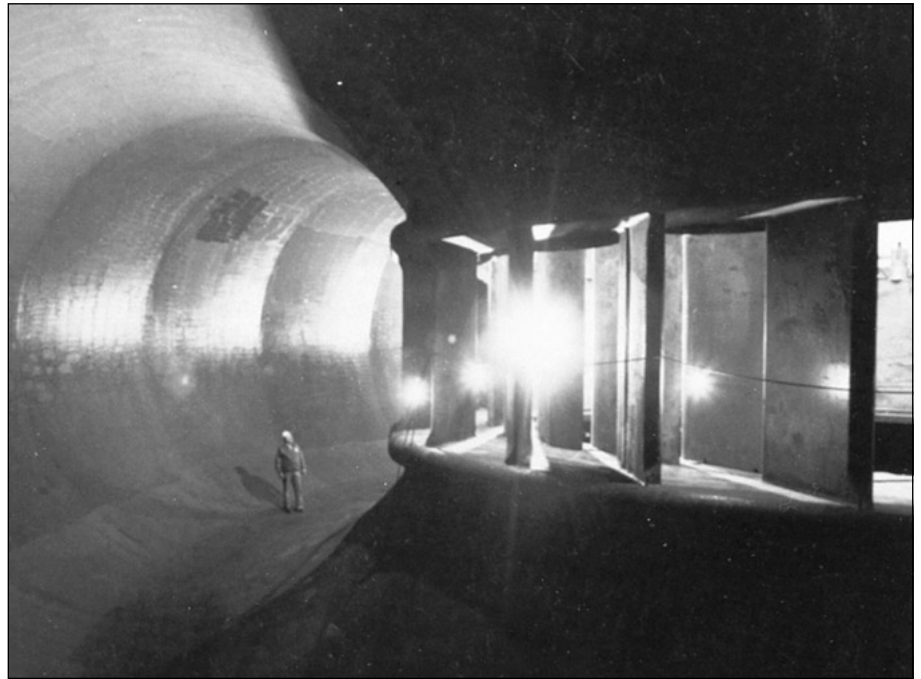


Fig. 11.25 Impulse turbine: (a) side view of wheel and jet; (b) top view of bucket; (c) typical velocity diagram.

Figure 11.26 shows Eq. (11.41) plotted for an ideal turbine ($\beta = 180^\circ$, $C_v = 1.0$) and for typical working conditions ($\beta = 160^\circ$, $C_v = 0.94$). The latter case predicts $\eta_{\max} = 85$ percent at $\phi = 0.47$, but the actual data for a 24-in Pelton wheel test are somewhat less efficient due to windage, mechanical friction, backsplashing, and nonuni-

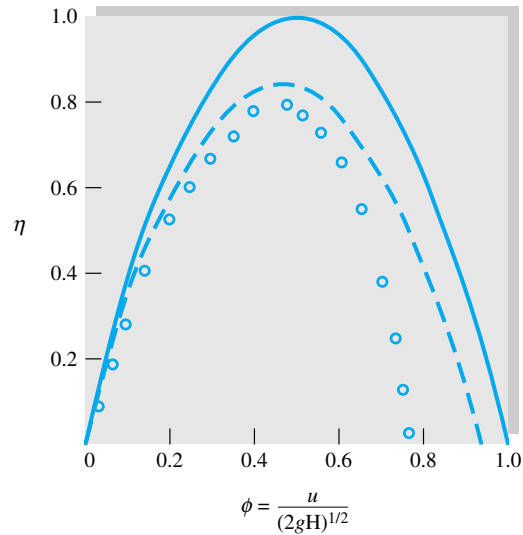


Fig. 11.26 Efficiency of an impulse turbine calculated from Eq. (11.41): solid curve = ideal, $\beta = 180^\circ$, $C_v = 1.0$; dashed curve = actual, $\beta = 160^\circ$, $C_v = 0.94$; open circles = data, Pelton wheel, diameter = 2 ft.

form bucket flow. For this test $\eta_{\max} = 80$ percent, and, generally speaking, an impulse turbine is not quite as efficient as the Francis or propeller turbines at their BEPs.

Figure 11.27 shows the optimum efficiency of the three turbine types, and the importance of the power specific speed N_{sp} as a selection tool for the designer. These efficiencies are optimum and are obtained in careful design of large machines.

The water power available to a turbine may vary due to either net-head or flow-rate changes, both of which are common in field installations such as hydroelectric plants. The demand for turbine power also varies from light to heavy, and the operating response is a change in the flow rate by adjustment of a gate valve or needle valve (Fig. 11.25a). As shown in Fig. 11.28, all three turbine types achieve fairly uniform efficiency as a function of the level of power being extracted. Especially effective is the adjustable-blade (Kaplan-type) propeller turbine, while the poorest is a fixed-blade propeller. The term *rated power* in Fig. 11.28 is the largest power delivery guaranteed by the manufacturer, as opposed to *normal power*, which is delivered at maximum efficiency.

For further details of design and operation of turbomachinery, the readable and interesting treatment in Ref. 33 is especially recommended. The feasibility of microhydropower is discussed in [26]. See also Refs. 27 and 28.

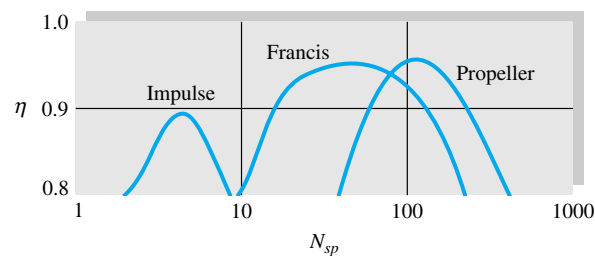


Fig. 11.27 Optimum efficiency of turbine designs.

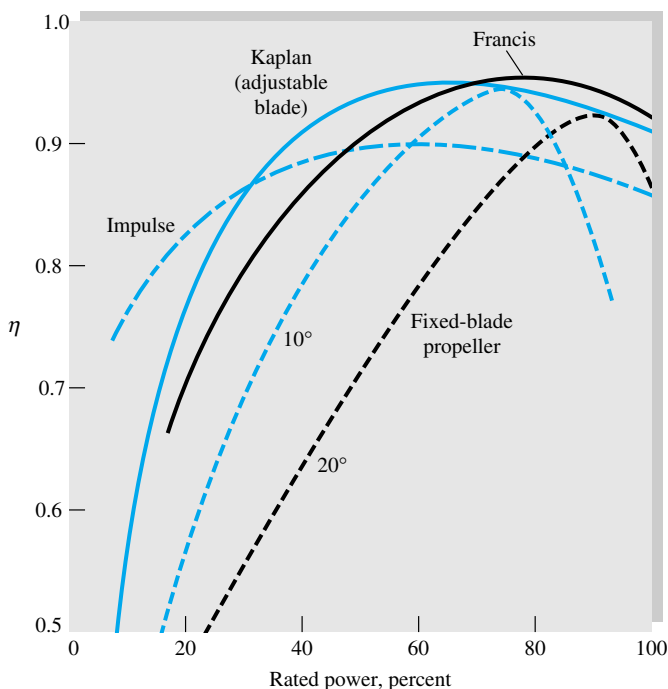


Fig. 11.28 Efficiency versus power level for various turbine designs at constant speed and head.

EXAMPLE 11.9

Investigate the possibility of using (a) a Pelton wheel similar to Fig. 11.26 or (b) the Francis turbine family of Fig. 11.21*d* to deliver 30,000 bhp from a net head of 1200 ft.

Solution

Part (a) From Fig. 11.27, the most efficient Pelton wheel occurs at about

$$N_{sp} \approx 4.5 = \frac{(r/\text{min})(30,000 \text{ bhp})^{1/2}}{(1200 \text{ ft})^{1.25}}$$

or $n = 183 \text{ r/min} = 3.06 \text{ r/s}$

From Fig. 11.26 the best operating point is

$$\phi \approx 0.47 = \frac{\pi D(3.06 \text{ r/s})}{[2(32.2)(1200)]^{1/2}}$$

or $D = 13.6 \text{ ft}$

Ans. (a)

This Pelton wheel is perhaps a little slow and a trifle large. You could reduce D and increase n by increasing N_{sp} to, say, 6 or 7 and accepting the slight reduction in efficiency. Or you could use a double-hung, two-wheel configuration, each delivering 15,000 bhp, which changes D and n by the factor $2^{1/2}$:

Double wheel: $n = (183)2^{1/2} = 260 \text{ r/min}$ $D = \frac{13.6}{2^{1/2}} = 9.6 \text{ ft}$ *Ans. (a)*

Part (b) The Francis wheel of Fig. 11.21*d* must have

$$N_{sp} = 29 = \frac{(\text{r/min})(30,000 \text{ bhp})^{1/2}}{(1200 \text{ ft})^{1.25}}$$

or
$$n = 1183 \text{ r/min} = 19.7 \text{ r/s}$$

Then the optimum power coefficient is

$$C_{p*} = 2.70 = \frac{P}{\rho n^3 D^5} = \frac{30,000(550)}{(1.94)(19.7)^3 D^5}$$

or
$$D^5 = 412 \quad D = 3.33 \text{ ft} = 40 \text{ in} \quad \text{Ans. (b)}$$

This is a faster speed than normal practice, and the casing would have to withstand 1200 ft of water or about 520 lbf/in² internal pressure, but the 40-in size is extremely attractive. Francis turbines are now being operated at heads up to 1500 ft.

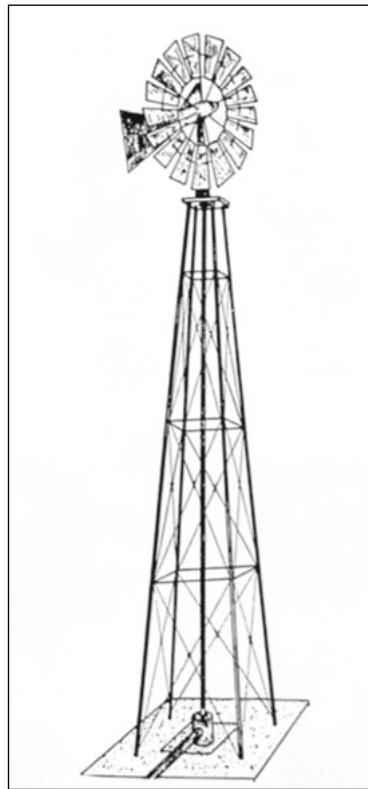
Wind Turbines

Wind energy has long been used as a source of mechanical power. The familiar four-bladed windmills of Holland, England, and the Greek islands have been used for centuries to pump water, grind grain, and saw wood. Modern research concentrates on the ability of wind turbines to generate electric power. Koepl [47] stresses the potential for propeller-type machines. Spera [49] gives a detailed discussion of the technical and economic feasibility of large-scale electric power generation by wind. See also Refs. 46, 48, and 50 to 52.

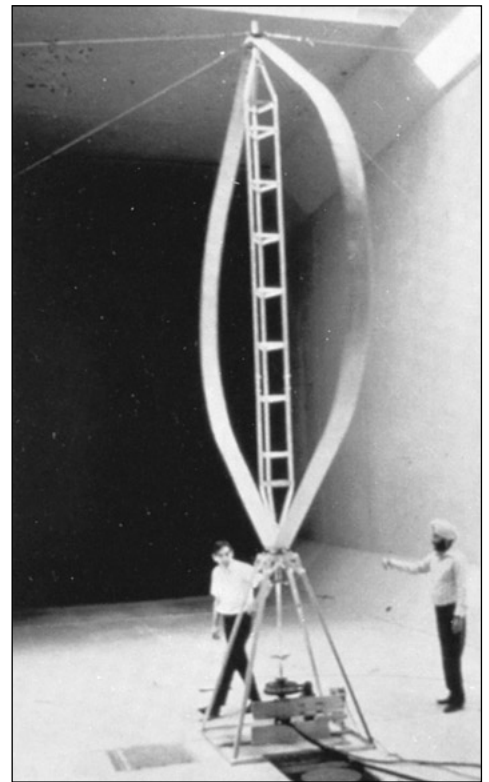
Some examples of wind turbine designs are shown in Fig. 11.29. The familiar American multiblade farm windmill (Fig. 11.29*a*) is of low efficiency, but thousands are in use as a rugged, reliable, and inexpensive way to pump water. A more efficient design is the propeller mill in Fig. 11.29*b*, similar to the pioneering Smith-Putnam 1250-kW two-bladed system which operated on Grampa's Knob, 12 mi west of Rutland, Vermont, from 1941 to 1945. The Smith-Putnam design broke because of inadequate blade strength, but it withstood winds up to 115 mi/h and its efficiency was amply demonstrated [47].

The Dutch, American multiblade, and propeller mills are examples of *horizontal-axis wind turbines* (HAWTs), which are efficient but somewhat awkward in that they require extensive bracing and gear systems when combined with an electric generator. Thus a competing family of *vertical-axis wind turbines* (VAWTs) has been proposed which simplifies gearing and strength requirements. Figure 11.29*c* shows the "egg-beater" VAWT invented by G. J. M. Darrieus in 1925, now used in several government-sponsored demonstration systems. To minimize centrifugal stresses, the twisted blades of the Darrieus turbine follow a *troposkien* curve formed by a chain anchored at two points on a spinning vertical rod.

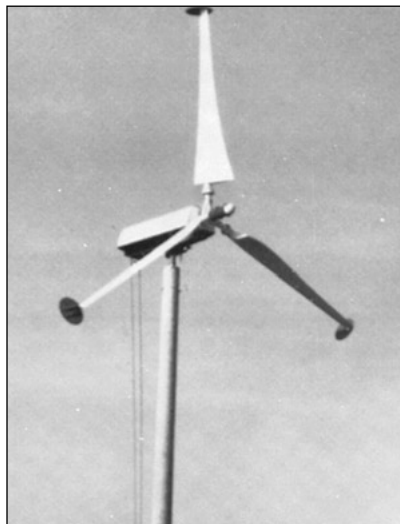
An alternative VAWT, simpler to construct than the troposkien, is the straight-bladed Darrieus-type turbine in Fig. 11.29*d*. This design, proposed by Reading University in England, has blades which pivot due to centrifugal action as wind speeds increase, thus limiting bending stresses.



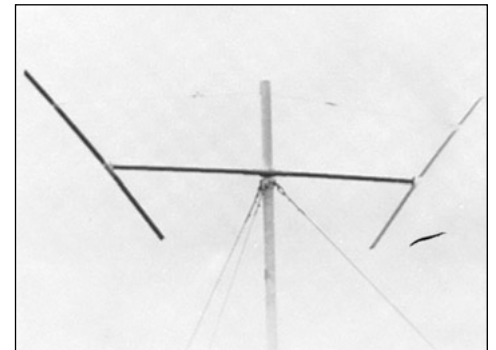
(a)



(c)



(b)



(d)

Fig. 11.29 Wind turbine designs: (a) the American multiblade farm HAWT; (b) propeller HAWT (Courtesy of Grumman Aerospace Corp.); (c) the Darrieus VAWT (Courtesy of National Research Council, Canada); (d) modified straight-blade Darrieus VAWT (Courtesy of Reading University—Nat'l Wind Power Ltd.).

Idealized Wind Turbine Theory

The ideal, frictionless efficiency of a propeller windmill was predicted by A. Betz in 1920, using the simulation shown in Fig. 11.30. The propeller is represented by an *actuator disk* which creates across the propeller plane a pressure discontinuity of area A and local velocity V . The wind is represented by a streamtube of approach velocity V_1 and a slower downstream wake velocity V_2 . The pressure rises to p_b just before the disk and drops to p_a just after, returning to free-stream pressure in the far wake. To hold the propeller rigid when it is extracting energy from the wind, there must be a leftward force F on its support, as shown.

A control-volume–horizontal-momentum relation applied between sections 1 and 2 gives

$$\sum F_x = -F = \dot{m}(V_2 - V_1)$$

A similar relation for a control volume just before and after the disk gives

$$\sum F_x = -F + (p_b - p_a)A = \dot{m}(V_a - V_b) = 0$$

Equating these two yields the propeller force

$$F = (p_b - p_a)A = \dot{m}(V_1 - V_2) \quad (11.42)$$

Assuming ideal flow, the pressures can be found by applying the incompressible Bernoulli relation up to the disk

$$\text{From 1 to } b: \quad p_\infty + \frac{1}{2}\rho V_1^2 = p_b + \frac{1}{2}\rho V^2$$

$$\text{From } a \text{ to 2:} \quad p_a + \frac{1}{2}\rho V^2 = p_\infty + \frac{1}{2}\rho V_2^2$$

Subtracting these and noting that $\dot{m} = \rho AV$ through the propeller, we can substitute for $p_b - p_a$ in Eq. (11.42) to obtain

$$p_b - p_a = \frac{1}{2}\rho(V_1^2 - V_2^2) = \rho V(V_1 - V_2)$$

$$\text{or} \quad V = \frac{1}{2}(V_1 + V_2) \quad (11.43)$$

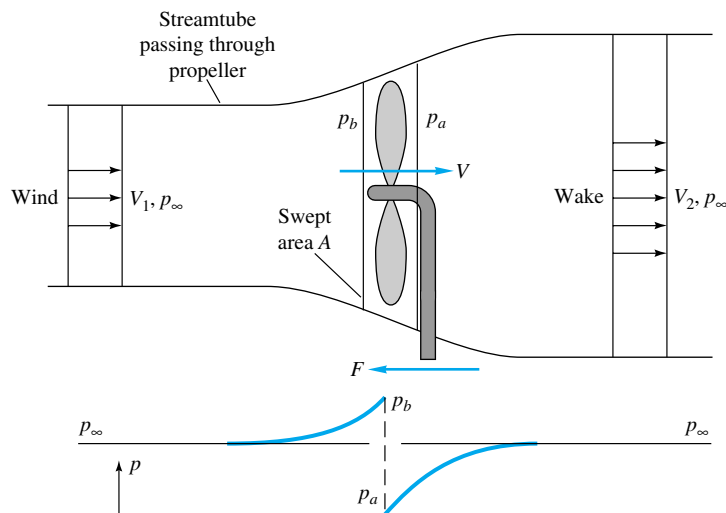


Fig. 11.30 Idealized actuator-disk and streamtube analysis of flow through a windmill.

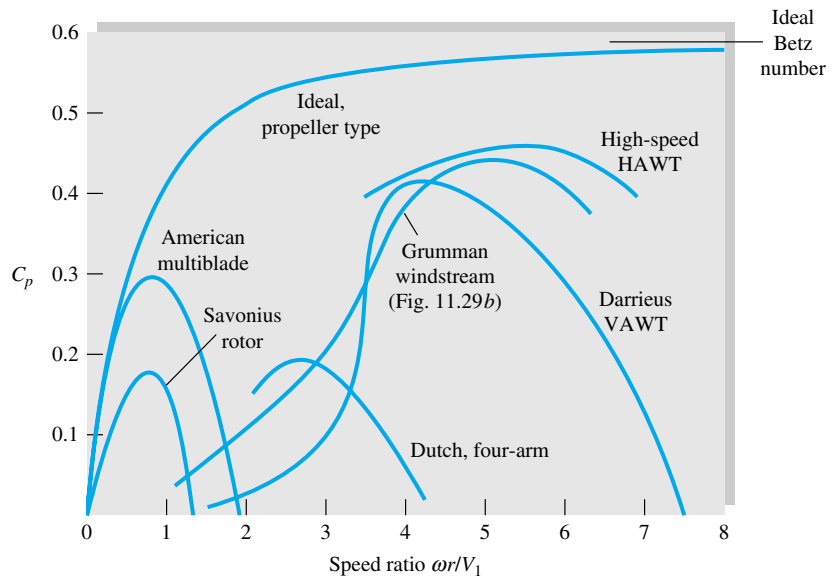


Fig. 11.31 Estimated performance of various wind turbine designs as a function of blade-tip speed ratio. (From Ref. 53.)

Continuity and momentum thus require that the velocity V through the disk equal the average of the wind and far-wake speeds.

Finally, the power extracted by the disk can be written in terms of V_1 and V_2 by combining Eqs. (11.42) and (11.43)

$$P = FV = \rho AV^2(V_1 - V_2) = \frac{1}{4}\rho A(V_1^2 - V_2^2)(V_1 + V_2) \quad (11.44)$$

For a given wind speed V_1 , we can find the maximum possible power by differentiating P with respect to V_2 and setting equal to zero. The result is

$$P = P_{\max} = \frac{8}{27}\rho AV_1^3 \quad \text{at } V_2 = \frac{1}{3}V_1 \quad (11.45)$$

which corresponds to $V = 2V_1/3$ through the disk.

The maximum available power to the propeller is the mass flow through the propeller times the total kinetic energy of the wind

$$P_{\text{avail}} = \frac{1}{2}\dot{m}V_1^2 = \frac{1}{2}\rho AV_1^3$$

Thus the maximum possible efficiency of an ideal frictionless wind turbine is usually stated in terms of the *power coefficient*

$$C_P = \frac{P}{\frac{1}{2}\rho AV_1^3} \quad (11.46)$$

Equation (11.45) states that the total power coefficient is

$$C_{P,\max} = \frac{16}{27} = 0.593 \quad (11.47)$$

This is called the *Betz number* and serves as an ideal with which to compare the actual performance of real windmills.

Figure 11.31 shows the measured power coefficients of various wind turbine designs. The independent variable is not V_2/V_1 (which is artificial and convenient only in

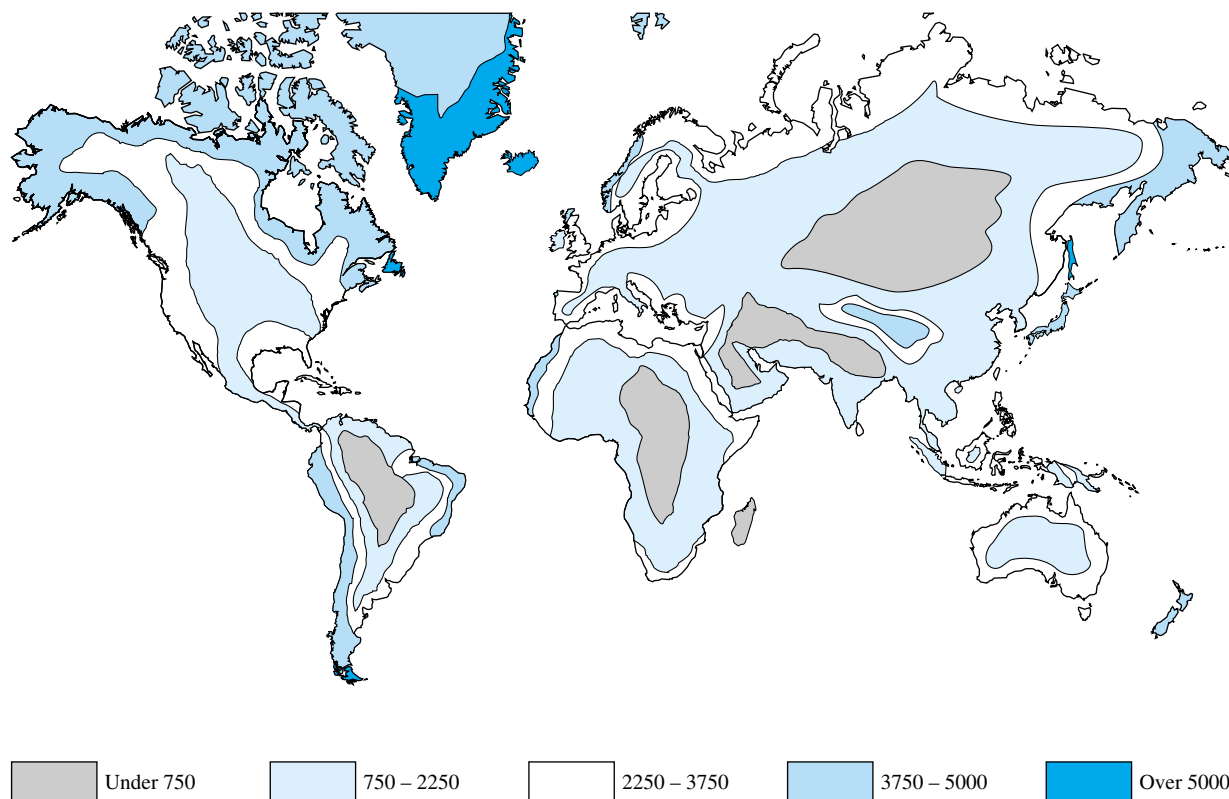


Fig. 11.32 World availability of land-based wind energy: estimated annual electric output in kWh/kW of a wind turbine rated at 11.2 m/s (25 mi/h). (From Ref. 54.)

the ideal theory) but the ratio of blade-tip speed ωr to wind speed. Note that the tip can move much faster than the wind, a fact disturbing to the laity but familiar to engineers in the behavior of iceboats and sailing vessels. The Darrieus has the many advantages of a vertical axis but has little torque at low speeds and also rotates more slowly at maximum power than a propeller, thus requiring a higher gear ratio for the generator. The Savonius rotor (Fig. 6.29*b*) has been suggested as a VAWT design because it produces power at very low wind speeds, but it is inefficient and susceptible to storm damage because it cannot be feathered in high winds.

As shown in Fig. 11.32, there are many areas of the world where wind energy is an attractive alternative. Greenland, Newfoundland, Argentina, Chile, New Zealand, Iceland, Ireland, and the United Kingdom have the highest prevailing winds, but Australia, e.g., with only moderate winds, has the potential to generate half its electricity with wind turbines [53]. In addition, since the ocean is generally even windier than the land, there are many island areas of high potential for wind power. There have also been proposals [47] for ocean-based floating windmill farms. The inexhaustible availability of the winds, coupled with improved low-cost turbine designs, indicates a bright future for this alternative.

Summary

Turbomachinery design is perhaps the most practical and most active application of the principles of fluid mechanics. There are billions of pumps and turbines in use in the world, and thousands of companies are seeking improvements. This chapter discusses both positive-displacement devices and, more extensively, rotodynamic machines. With the centrifugal pump as an example, the basic concepts of torque, power, head, flow rate, and efficiency are developed for a turbomachine. Nondimensionalization leads to the pump similarity rules and some typical dimensionless performance curves for axial and centrifugal machines. The single most useful pump parameter is found to be the specific speed, which delineates the type of design needed. An interesting design application is the theory of pumps combined in series and in parallel.

Turbines extract energy from flowing fluids and are of two types: impulse turbines, which convert the momentum of a high-speed stream, and reaction turbines, where the pressure drop occurs within the blade passages in an internal flow. By analogy with pumps, the power specific speed is important for turbines and is used to classify them into impulse, Francis, and propeller-type designs. A special case of reaction turbine with unconfined flow is the wind turbine. Several types of windmills are discussed and their relative performances compared.

Problems

Most of the problems herein are fairly straightforward. More difficult or open-ended assignments are labeled with an asterisk. Problems labeled with an EES icon will benefit from the use of the Engineering Equations Solver (EES), while problems labeled with a computer icon may require the use of a computer. The standard end-of-chapter problems 11.1 to 11.103 (categorized in the problem list below) are followed by word problems W11.1 to W11.10, comprehensive problems C11.1 to C11.3, and design project D11.1.

Problem distribution

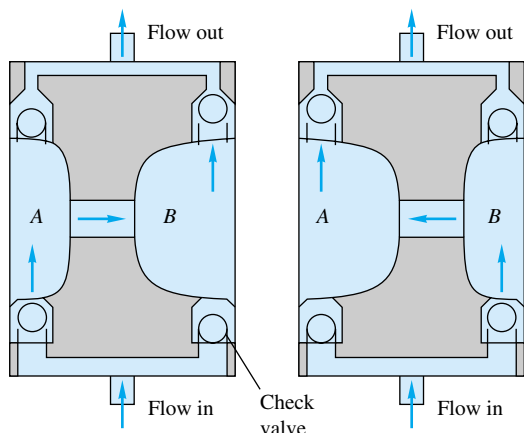
Section	Topic	Problems
11.1	Introduction and classification	11.1–11.14
11.2	Centrifugal pump theory	11.15–11.21
11.3	Pump performance and similarity rules	11.22–11.41
11.3	Net positive-suction head	11.42–11.44
11.4	Specific speed: Mixed- and axial-flow pumps	11.45–11.62
11.5	Matching pumps to system characteristics	11.63–11.73
11.5	Pumps in parallel or series	11.74–11.81
11.5	Pump instability	11.82–11.83
11.6	Reaction and impulse turbines	11.84–11.99
11.6	Wind turbines	11.100–11.103

- P11.1** Describe the geometry and operation of a peristaltic positive-displacement pump which occurs in nature.
- P11.2** What would be the technical classification of the following turbomachines: (a) a household fan, (b) a windmill, (c) an aircraft propeller, (d) a fuel pump in a car, (e) an eductor, (f) a fluid-coupling transmission, and (g) a power plant steam turbine?

- P11.3** A PDP can deliver almost any fluid, but there is always a limiting very high viscosity for which performance will deteriorate. Can you explain the probable reason?
- P11.4** Figure 11.2c shows a double-screw pump. Sketch a single-screw pump and explain its operation. How did Archimedes' screw pump operate?
- P11.5** What type of pump is shown in Fig. P11.5? How does it operate?



- P11.6** Figure P11.6 shows two points a half-period apart in the operation of a pump. What type of pump is this? How does it work? Sketch your best guess of flow rate versus time for a few cycles.
- P11.7** A piston PDP has a 5-in diameter and a 2-in stroke and operates at 750 r/min with 92 percent volumetric efficiency. (a) What is its delivery, in gal/min? (b) If the pump delivers SAE 10W oil at 20°C against a head of 50 ft, what horsepower is required when the overall efficiency is 84 percent?



P11.6

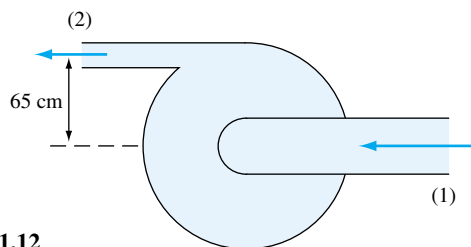
P11.8 A centrifugal pump delivers 550 gal/min of water at 20°C when the brake horsepower is 22 and the efficiency is 71 percent. (a) Estimate the head rise in ft and the pressure rise in lbf/in². (b) Also estimate the head rise and horsepower if instead the delivery is 550 gal/min of gasoline at 20°C.

P11.9 Figure P11.9 shows the measured performance of the Vickers model PVQ40 piston pump when delivering SAE 10W oil at 180°F ($\rho \approx 910 \text{ kg/m}^3$). Make some general observations about these data vis-à-vis Fig. 11.2 and your intuition about the behavior of piston pumps.

P11.10 Suppose that the piston pump of Fig. P11.9 is used to deliver 15 gal/min of water at 20°C using 20 brake horsepower. Neglecting Reynolds-number effects, use the figure to estimate (a) the speed in r/min and (b) the pressure rise in lbf/in².

P11.11 A pump delivers 1500 L/min of water at 20°C against a pressure rise of 270 kPa. Kinetic- and potential-energy changes are negligible. If the driving motor supplies 9 kW, what is the overall efficiency?

P11.12 In a test of the centrifugal pump shown in Fig. P11.12, the following data are taken: $p_1 = 100 \text{ mmHg}$ (vacuum) and $p_2 = 500 \text{ mmHg}$ (gage). The pipe diameters are $D_1 = 12 \text{ cm}$ and $D_2 = 5 \text{ cm}$. The flow rate is 180 gal/min of light oil ($\text{SG} = 0.91$). Estimate (a) the head developed,



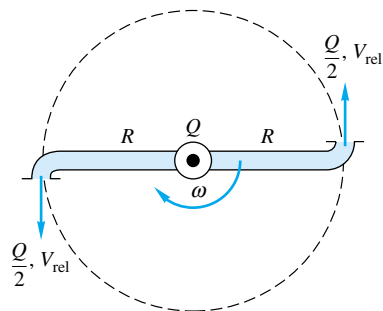
P11.12

in meters; and (b) the input power required at 75 percent efficiency.

P11.13 A 20-hp pump delivers 400 gal/min of gasoline at 20°C with 75 percent efficiency. What head and pressure rise result across the pump?

P11.14 A pump delivers gasoline at 20°C and 12 m³/h. At the inlet $p_1 = 100 \text{ kPa}$, $z_1 = 1 \text{ m}$, and $V_1 = 2 \text{ m/s}$. At the exit $p_2 = 500 \text{ kPa}$, $z_2 = 4 \text{ m}$, and $V_2 = 3 \text{ m/s}$. How much power is required if the motor efficiency is 75 percent?

P11.15 A lawn sprinkler can be used as a simple turbine. As shown in Fig. P11.15, flow enters normal to the paper in the center and splits evenly into $Q/2$ and V_{rel} leaving each nozzle. The arms rotate at angular velocity ω and do work on a shaft. Neglecting friction, find an expression for the power delivered to the shaft. Find the rotation rate for which the power is a maximum.

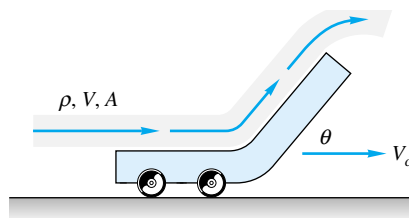


P11.15

P11.16 For the “sprinkler turbine” of Fig. P11.15, let $R = 18 \text{ cm}$, with total flow rate of 14 m³/h of water at 20°C. If the nozzle exit diameter is 8 mm, estimate (a) the maximum power delivered in W and (b) the appropriate rotation rate in r/min.

P11.17 A centrifugal pump has $d_1 = 7 \text{ in}$, $d_2 = 13 \text{ in}$, $b_1 = 4 \text{ in}$, $b_2 = 3 \text{ in}$, $\beta_1 = 25^\circ$, and $\beta_2 = 40^\circ$ and rotates at 1160 r/min. If the fluid is gasoline at 20°C and the flow enters the blades radially, estimate the theoretical (a) flow rate in gal/min, (b) horsepower, and (c) head in ft.

P11.18 A jet of velocity V strikes a vane which moves to the right at speed V_c , as in Fig. P11.18. The vane has a turning angle θ .



P11.18

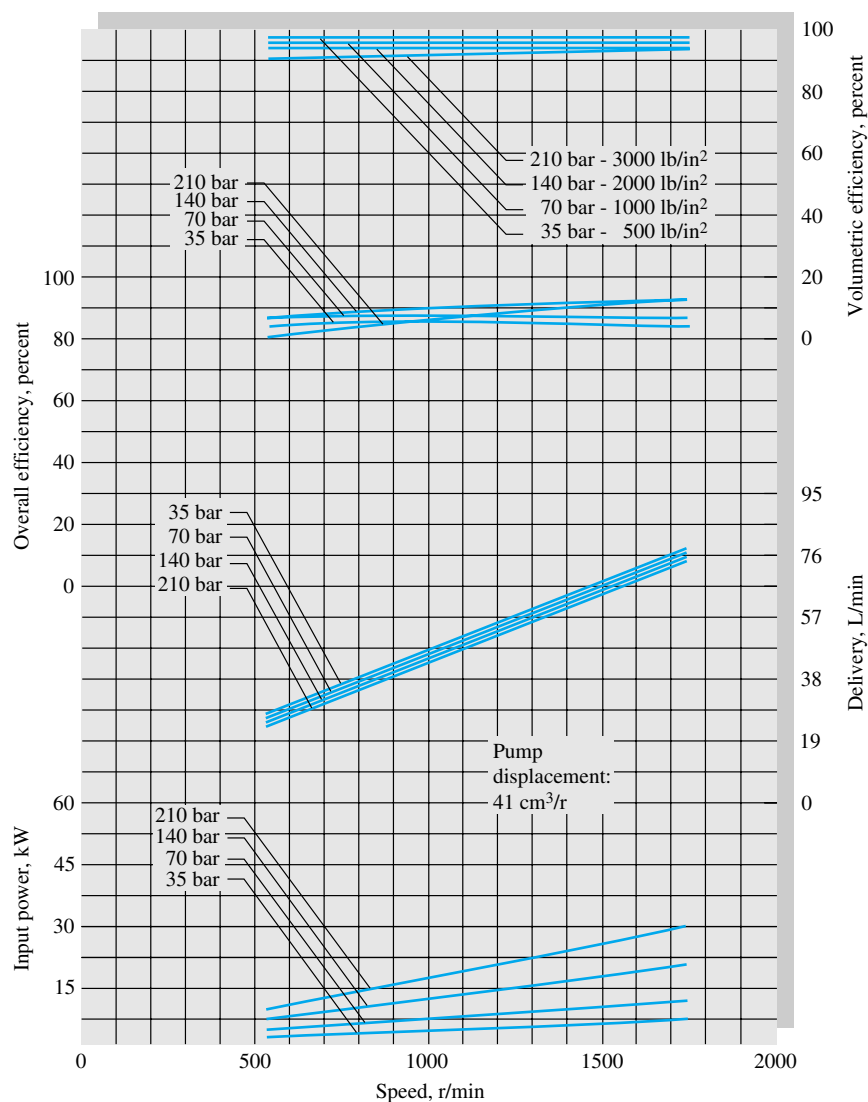
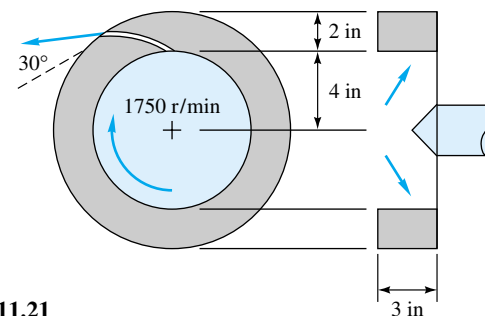


Fig. P11.9 Performance of the model PVQ40 piston pump delivering SAE 10W oil at 180°F. (Courtesy of Vickers Inc., PDN/PACE Division.)

- Derive an expression for the power delivered to the vane by the jet. For what vane speed is the power maximum?
- P11.19** A centrifugal pump has $r_2 = 9$ in, $b_2 = 2$ in, and $\beta_2 = 35^\circ$ and rotates at 1060 r/min. If it generates a head of 180 ft, determine the theoretical (a) flow rate in gal/min and (b) horsepower. Assume near-radial entry flow.
- P11.20** Suppose that Prob. 11.19 is reversed into a statement of the theoretical power $P_w \approx 153$ hp. Can you then compute the theoretical (a) flow rate and (b) head? Explain and resolve the difficulty which arises.
- P11.21** The centrifugal pump of Fig. P11.21 develops a flow rate of 4200 gal/min of gasoline at 20°C with near-radial absolute



P11.21

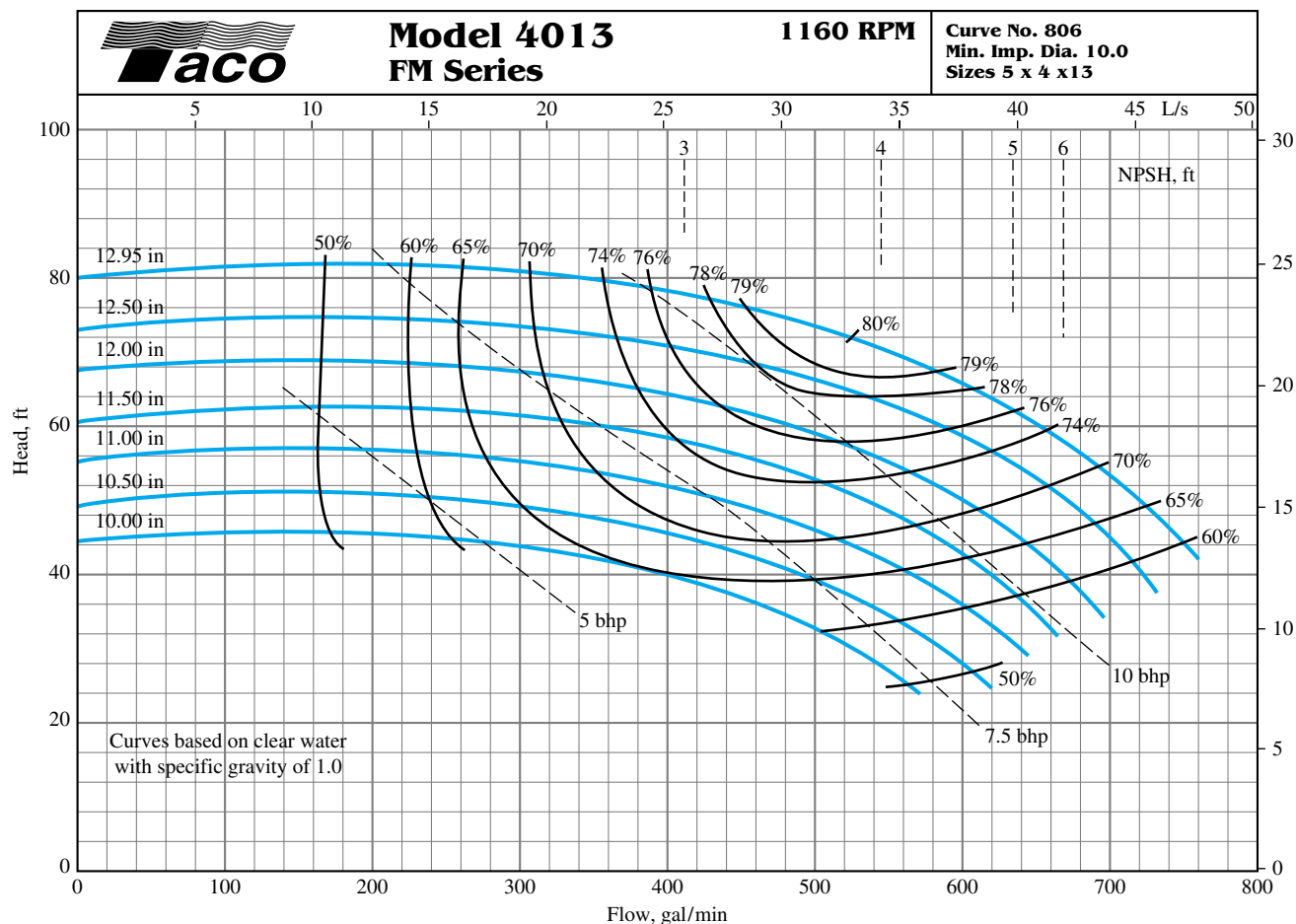


Fig. P11.24 Performance data for a centrifugal pump. (Courtesy of Taco, Inc., Cranston, Rhode Island.)

inflow. Estimate the theoretical (a) horsepower, (b) head rise, and (c) appropriate blade angle at the inner radius.

- P11.22** A 37-cm-diameter centrifugal pump, running at 2140 r/min with water at 20°C, produces the following performance data:

Q , m ³ /s	0.0	0.05	0.10	0.15	0.20	0.25	0.30
H , m	105	104	102	100	95	85	67
P , kW	100	115	135	171	202	228	249

(a) Determine the best efficiency point. (b) Plot C_H versus C_Q . (c) If we desire to use this same pump family to deliver 7000 gal/min of kerosine at 20°C at an input power of 400 kW, what pump speed (in r/min) and impeller size (in cm) are needed? What head will be developed?

- P11.23** If the 38-in-diameter pump of Fig. 11.7b is used to deliver 20°C kerosine at 850 r/min and 22,000 gal/min, what (a) head and (b) brake horsepower will result?

- P11.24** Figure P11.24 shows performance data for the Taco, Inc., model 4013 pump. Compute the ratios of measured shut-off head to the ideal value U^2/g for all seven impeller sizes. Determine the average and standard deviation of this ratio and compare it to the average for the six impellers in Fig. 11.7.

- P11.25** At what speed in r/min should the 35-in-diameter pump of Fig. 11.7b be run to produce a head of 400 ft at a discharge of 20,000 gal/min? What brake horsepower will be required? *Hint:* Fit $H(Q)$ to a formula.

- P11.26** Determine if the seven Taco, Inc., pump sizes in Fig. P11.24 can be collapsed into a single dimensionless chart

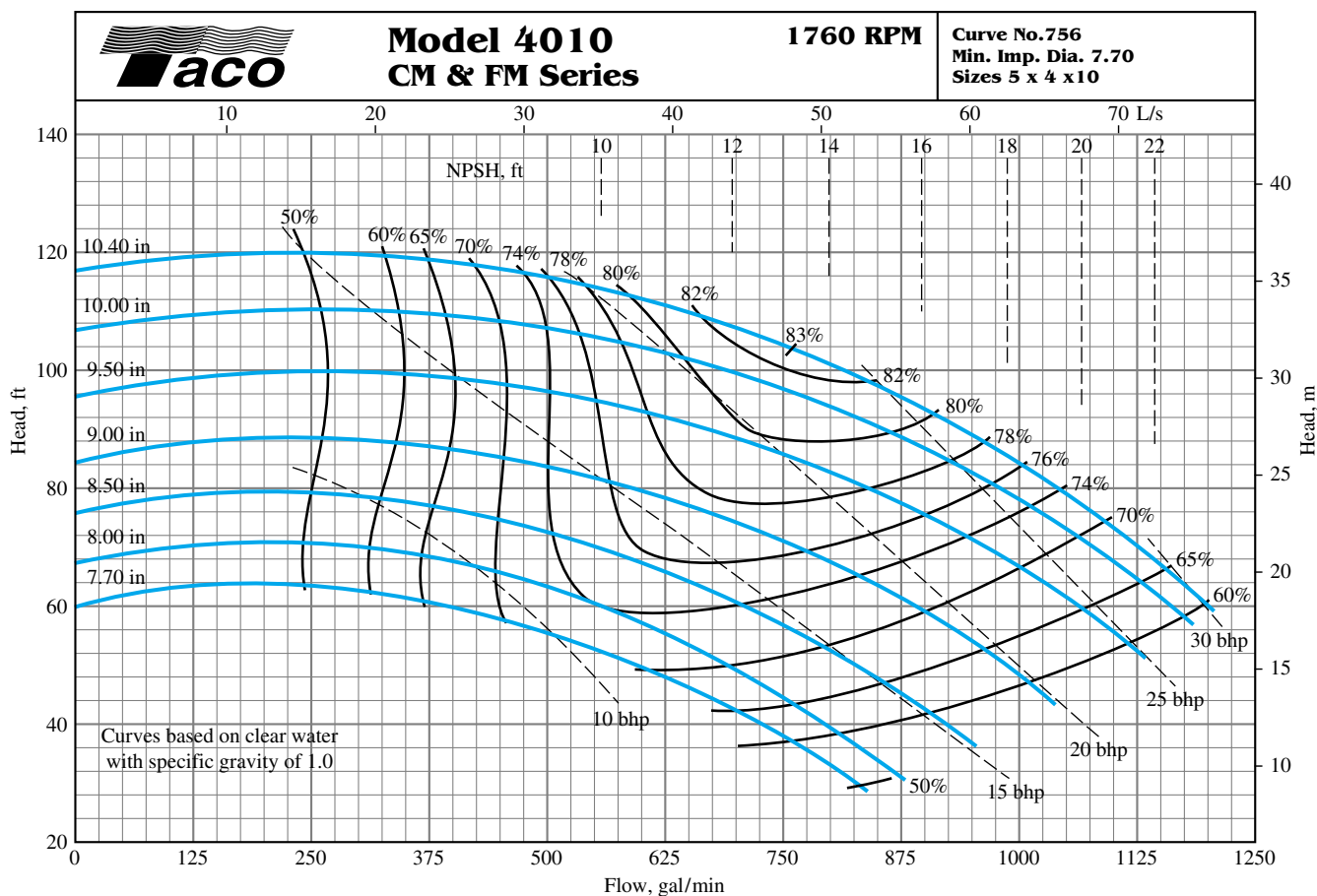


Fig. P11.31 Performance data for a family of centrifugal pump impellers. (Courtesy of Taco, Inc., Cranston, Rhode Island.)

of C_H , C_P , and η versus C_Q , as in Fig. 11.8. Comment on the results.

P11.27 The 12-in pump of Fig. P11.24 is to be scaled up in size to provide a head of 90 ft and a flow rate of 1000 gal/min at BEP. Determine the correct (a) impeller diameter, (b) speed in r/min, and (c) horsepower required.

P11.28 Tests by the Byron Jackson Co. of a 14.62-in-diameter centrifugal water pump at 2134 r/min yield the following data:

Q , ft ³ /s	0	2	4	6	8	10
H , ft	340	340	340	330	300	220
bhp	135	160	205	255	330	330

What is the BEP? What is the specific speed? Estimate the maximum discharge possible.

P11.29 If the scaling laws are applied to the pump of Prob. 11.28 for the same impeller diameter, determine (a) the speed for which the shutoff head will be 280 ft, (b) the speed for which the BEP flow rate will be 8.0 ft³/s, and (c) the speed for which the BEP conditions will require 80 hp.

P11.30 A pump from the same family as Prob. 11.28 is built with $D = 18$ in and a BEP power of 250 hp for gasoline (not water). Using the scaling laws, estimate the resulting (a) speed in r/min, (b) flow rate at BEP, and (c) shutoff head.

P11.31 Figure P11.31 shows performance data for the Taco, Inc., model 4010 pump. Compute the ratios of measured shutoff head to the ideal value U^2/g for all seven impeller sizes. Determine the average and standard deviation of this ratio, and compare it to the average of 0.58 ± 0.02 for the seven impellers in Fig. P11.24. Comment on your results.

P11.32 Determine if the seven Taco, Inc., impeller sizes in Fig. P11.31 can be collapsed into a single dimensionless chart of C_H , C_P , and η versus C_Q , as in Fig. 11.8. Comment on the results.

P11.33 Clearly the maximum efficiencies of the pumps in Figs. P11.24 and P11.31 decrease with impeller size. Compare η_{\max} for these two pump families with both the Moody and the Anderson correlations, Eqs. (11.29). Use the central impeller size as a comparison point.

P11.34 You are asked to consider a pump geometrically similar to the 9-in-diameter pump of Fig. P11.31 to deliver 1200 gal/min at 1500 r/min. Determine the appropriate (a) impeller diameter, (b) BEP horsepower, (c) shutoff head, and (d) maximum efficiency. The fluid is kerosine, not water.

P11.35 An 18-in-diameter centrifugal pump, running at 880 r/min with water at 20°C, generates the following performance data:

Q , gal/min	0.0	2000	4000	6000	8000	10,000
H , ft	92	89	84	78	68	50
P , hp	100	112	130	143	156	163

Determine (a) the BEP, (b) the maximum efficiency, and (c) the specific speed. (d) Plot the required input power versus the flow rate.

P11.36 Plot the dimensionless performance curves for the pump of Prob. 11.35 and compare with Fig. 11.8. Find the appropriate diameter in inches and speed in r/min for a geometrically similar pump to deliver 400 gal/min against a head of 200 ft. What brake horsepower would be required?

P11.37 The efficiency of a centrifugal pump can be approximated by the curve fit $\eta \approx aQ - bQ^3$, where a and b are constants. For this approximation, (a) what is the ratio of Q^* at BEP to Q_{\max} ? If the maximum efficiency is 88 percent, what is the efficiency at (b) $\frac{1}{3}Q_{\max}$ and (c) $\frac{4}{3}Q^*$?

P11.38 A 6.85-in pump, running at 3500 r/min, has the following measured performance for water at 20°C:

Q , gal/min	50	100	150	200	250	300	350	400	450
H , ft	201	200	198	194	189	181	169	156	139
η , %	29	50	64	72	77	80	81	79	74

(a) Estimate the horsepower at BEP. If this pump is rescaled in water to provide 20 bhp at 3000 r/min, determine the appropriate (b) impeller diameter, (c) flow rate, and (d) efficiency for this new condition.

P11.39 The Allis-Chalmers D30LR centrifugal compressor delivers 33,000 ft³/min of SO₂ with a pressure change from

14.0 to 18.0 lbf/in² absolute using an 800-hp motor at 3550 r/min. What is the overall efficiency? What will the flow rate and Δp be at 3000 r/min? Estimate the diameter of the impeller.

P11.40 The specific speed N_s , as defined by Eqs. (11.30), does not contain the impeller diameter. How then should we size the pump for a given N_s ? Logan [7] suggests a parameter called the *specific diameter* D_s , which is a dimensionless combination of Q , gH , and D . (a) If D_s is proportional to D , determine its form. (b) What is the relationship, if any, of D_s to C_{Q^*} , C_{H^*} , and C_{P^*} ? (c) Estimate D_s for the two pumps of Figs. 11.8 and 11.13.

P11.41 It is desired to build a centrifugal pump geometrically similar to that of Prob. 11.28 to deliver 6500 gal/min of gasoline at 20°C at 1060 r/min. Estimate the resulting (a) impeller diameter, (b) head, (c) brake horsepower, and (d) maximum efficiency.

P11.42 An 8-in model pump delivering 180°F water at 800 gal/min and 2400 r/min begins to cavitate when the inlet pressure and velocity are 12 lbf/in² absolute and 20 ft/s, respectively. Find the required NPSH of a prototype which is 4 times larger and runs at 1000 r/min.

P11.43 The 28-in-diameter pump in Fig. 11.7a at 1170 r/min is used to pump water at 20°C through a piping system at 14,000 gal/min. (a) Determine the required brake horsepower. The average friction factor is 0.018. (b) If there is 65 ft of 12-in-diameter pipe upstream of the pump, how far below the surface should the pump inlet be placed to avoid cavitation?

P11.44 The pump of Prob. 11.28 is scaled up to an 18-in diameter, operating in water at best efficiency at 1760 r/min. The measured NPSH is 16 ft, and the friction loss between the inlet and the pump is 22 ft. Will it be sufficient to avoid cavitation if the pump inlet is placed 9 ft below the surface of a sea-level reservoir?

P11.45 Determine the specific speeds of the seven Taco, Inc., pump impellers in Fig. P11.24. Are they appropriate for centrifugal designs? Are they approximately equal within experimental uncertainty? If not, why not?

P11.46 The answer to Prob. 11.40 is that the dimensionless “specific diameter” takes the form $D_s = D(gH^*)^{1/4}/Q^{*1/2}$, evaluated at the BEP. Data collected by the author for 30 different pumps indicate, in Fig. P11.46, that D_s correlates well with specific speed N_s . Use this figure to estimate the appropriate impeller diameter for a pump which delivers 20,000 gal/min of water and a head of 400 ft when running at 1200 r/min. Suggest a curve-fit formula to the data. *Hint:* Use a hyperbolic formula.

P11.47 A typical household basement sump pump provides a discharge of 5 gal/min against a head of 15 ft. Estimate (a) the maximum efficiency and (b) the minimum horsepower required to drive such a pump at 1750 r/min.

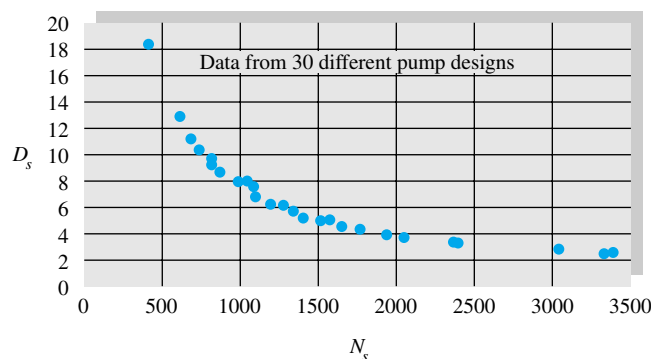


Fig. P11.46 Specific diameter at BEP for 30 commercial pumps.

P11.48 Compute the specific speeds for the pumps in Probs. 11.28, 11.35, and 11.38 plus the median sizes in Figs. P11.24 and P11.31. Then determine if their maximum efficiencies match the values predicted in Fig. 11.14.

P11.49 Data collected by the author for flow coefficient at BEP for 30 different pumps are plotted versus specific speed in Fig. P11.49. Determine if the values of C_Q^* for the five pumps in Prob. 11.48 also fit on this correlation. If so, suggest a curve-fitted formula for the data.

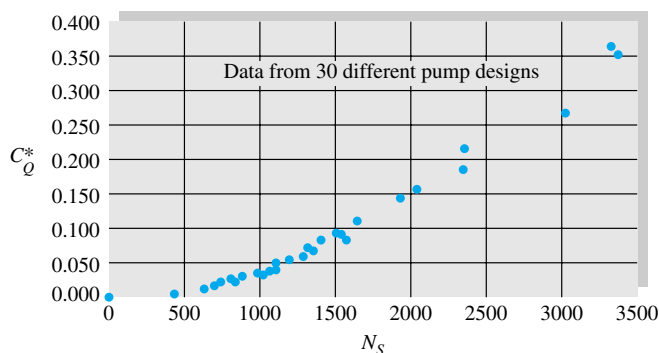


Fig. P11.49 Flow coefficient at BEP for 30 commercial pumps.

P11.50 Data collected by the author for power coefficient at BEP for 30 different pumps are plotted versus specific speed in Fig. P11.50. Determine if the values of C_P^* for the five pumps in Prob. 11.48 also fit on this correlation. If so, suggest a curve-fitted formula for the data.

P11.51 An axial-flow pump delivers $40 \text{ ft}^3/\text{s}$ of air which enters at 20°C and 1 atm. The flow passage has a 10-in outer radius and an 8-in inner radius. Blade angles are $\alpha_1 = 60^\circ$ and $\beta_2 = 70^\circ$, and the rotor runs at 1800 r/min. For the first stage compute (a) the head rise and (b) the power required.

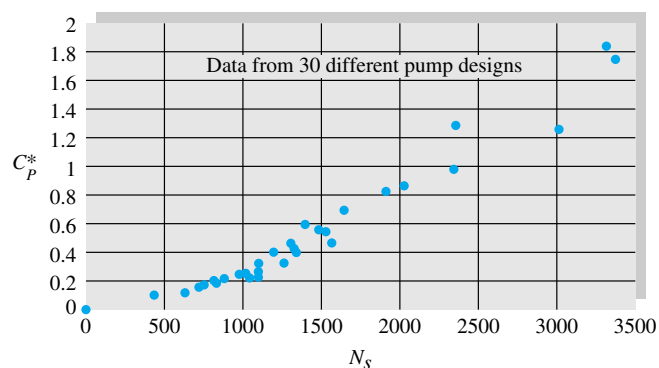


Fig. P11.50 Power coefficient at BEP for 30 commercial pumps.

P11.52 An axial-flow fan operates in sea-level air at 1200 r/min and has a blade-tip diameter of 1 m and a root diameter of 80 cm. The inlet angles are $\alpha_1 = 55^\circ$ and $\beta_1 = 30^\circ$, while at the outlet $\beta_2 = 60^\circ$. Estimate the theoretical values of the (a) flow rate, (b) horsepower, and (c) outlet angle α_2 .

P11.53 If the axial-flow pump of Fig. 11.13 is used to deliver 70,000 gal/min of 20°C water at 1170 r/min, estimate (a) the proper impeller diameter, (b) the shutoff head, (c) the shutoff horsepower, and (d) Δp at best efficiency.

P11.54 The Colorado River Aqueduct uses Worthington Corp. pumps which deliver $200 \text{ ft}^3/\text{s}$ at 450 r/min against a head of 440 ft. What types of pump are these? Estimate the impeller diameter.

P11.55 We want to pump 70°C water at 20,000 gal/min and 1800 r/min. Estimate the type of pump, the horsepower required, and the impeller diameter if the required pressure rise for one stage is (a) 170 kPa and (b) 1350 kPa.

P11.56 A pump is needed to deliver 40,000 gal/min of gasoline at 20°C against a head of 90 ft. Find the impeller size, speed, and brake horsepower needed to use the pump families of (a) Fig. 11.8 and (b) Fig. 11.13. Which is the better design?

P11.57 Performance data for a 21-in-diameter air blower running at 3550 r/min are as follows:

Δp , inH ₂ O	29	30	28	21	10
Q , ft ³ /min	500	1000	2000	3000	4000
bhp	6	8	12	18	25

Note the fictitious expression of pressure rise in terms of water rather than air. What is the specific speed? How does the performance compare with Fig. 11.8? What are C_Q^* , C_H^* , and C_P^* ?

P11.58 The Worthington Corp. model A-12251 water pump, operating at maximum efficiency, produces 53 ft of head at 3500 r/min, 1.1 bhp at 3200 r/min, and 60 gal/min at 2940 r/min. What type of pump is this? What is its efficiency, and how does this compare with Fig. 11.14? Estimate the impeller diameter.

P11.59 Suppose it is desired to deliver 700 ft³/min of propane gas (molecular weight = 44.06) at 1 atm and 20°C with a single-stage pressure rise of 8.0 inH₂O. Determine the appropriate size and speed for using the pump families of (a) Prob. 11.57 and (b) Fig. 11.13. Which is the better design?

P11.60 A 45-hp pump is desired to generate a head of 200 ft when running at BEP with 20°C gasoline at 1200 r/min. Using the correlations in Figs. P11.49 and P11.50, determine the appropriate (a) specific speed, (b) flow rate, and (c) impeller diameter.

P11.61 A mine ventilation fan, running at 295 r/min, delivers 500 m³/s of sea-level air with a pressure rise of 1100 Pa. Is this fan axial, centrifugal, or mixed? Estimate its diameter in ft. If the flow rate is increased 50 percent for the same diameter, by what percentage will the pressure rise change?

P11.62 The actual mine ventilation fan discussed in Prob. 11.61 had a diameter of 20 ft [20, p. 339]. What would be the proper diameter for the pump family of Fig. 11.14 to provide 500 m³/s at 295 r/min and BEP? What would be the resulting pressure rise in Pa?

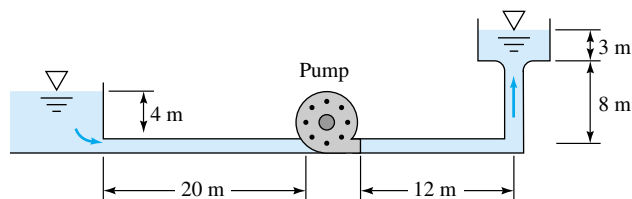
P11.63 The 36.75-in pump in Fig. 11.7a at 1170 r/min is used to pump water at 60°F from a reservoir through 1000 ft of 12-in-ID galvanized-iron pipe to a point 200 ft above the reservoir surface. What flow rate and brake horsepower will result? If there is 40 ft of pipe upstream of the pump, how far below the surface should the pump inlet be placed to avoid cavitation?

P11.64 In Prob. 11.63 the operating point is off design at an efficiency of only 77 percent. Is it possible, with the similarity rules, to change the pump rotation speed to deliver the water near BEP? Explain your results.

P11.65 The 38-in pump of Fig. 11.7a is used in series to lift 20°C water 3000 ft through 4000 ft of 18-in-ID cast-iron pipe. For most efficient operation, how many pumps in series are needed if the rotation speed is (a) 710 r/min and (b) 1200 r/min?

P11.66 It is proposed to run the pump of Prob. 11.35 at 880 r/min to pump water at 20°C through the system in Fig. P11.66. The pipe is 20-cm-diameter commercial steel. What flow rate in ft³/min will result? Is this an efficient application?

P11.67 The pump of Prob. 11.35, running at 880 r/min, is to pump water at 20°C through 75 m of horizontal galvanized-iron pipe. All other system losses are neglected.



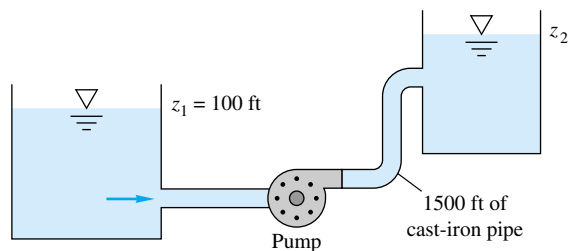
P11.66

Determine the flow rate and input power for (a) pipe diameter = 20 cm and (b) the pipe diameter found to yield maximum pump efficiency.

P11.68 A 24-in pump is homologous to the 32-in pump in Fig. 11.7a. At 1400 r/min this pump delivers 12,000 gal/min of water from one reservoir through a long pipe to another 50 ft higher. What will the flow rate be if the pump speed is increased to 1750 r/min? Assume no change in pipe friction factor or efficiency.

P11.69 The pump of Prob. 11.38, running at 3500 r/min, is used to deliver water at 20°C through 600 ft of cast-iron pipe to an elevation 100 ft higher. Determine (a) the proper pipe diameter for BEP operation and (b) the flow rate which results if the pipe diameter is 3 in.

P11.70 The pump of Prob. 11.28, operating at 2134 r/min, is used with 20°C water in the system of Fig. P11.70. (a) If it is operating at BEP, what is the proper elevation z_2 ? (b) If $z_2 = 225$ ft, what is the flow rate if $d = 8$ in.?



P11.70

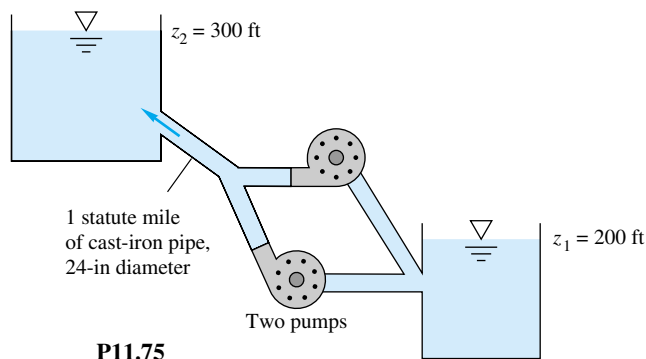
P11.71 The pump of Prob. 11.38, running at 3500 r/min, delivers water at 20°C through 7200 ft of horizontal 5-in-diameter commercial-steel pipe. There are a sharp entrance, sharp exit, four 90° elbows, and a gate valve. Estimate (a) the flow rate if the valve is wide open and (b) the valve closing percentage which causes the pump to operate at BEP. (c) If the latter condition holds continuously for 1 year, estimate the energy cost at 10 ¢/kWh.

P11.72 Performance data for a small commercial pump are as follows:

Q , gal/min	0	10	20	30	40	50	60	70
H , ft	75	75	74	72	68	62	47	24

This pump supplies 20°C water to a horizontal $\frac{5}{8}$ -in-diameter garden hose ($\epsilon \approx 0.01$ in) which is 50 ft long. Estimate (a) the flow rate and (b) the hose diameter which would cause the pump to operate at BEP.

- P11.73** The piston pump of Fig. P11.9 is run at 1500 r/min to deliver SAE 10W oil through 100 m of vertical 2-cm-diameter wrought-iron pipe. If other system losses are neglected, estimate (a) the flow rate, (b) the pressure rise, and (c) the power required.
- P11.74** The 32-in pump in Fig. 11.7a is used at 1170 r/min in a system whose head curve is H_s (ft) = $100 + 1.5Q^2$, with Q in thousands of gallons of water per minute. Find the discharge and brake horsepower required for (a) one pump, (b) two pumps in parallel, and (c) two pumps in series. Which configuration is best?
- P11.75** Two 35-in pumps from Fig. 11.7b are installed in parallel for the system of Fig. P11.75. Neglect minor losses. For water at 20°C, estimate the flow rate and power required if (a) both pumps are running and (b) one pump is shut off and isolated.

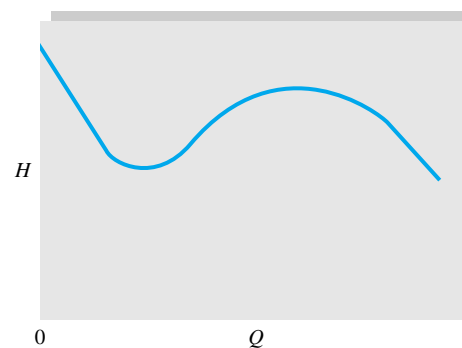


- P11.76** Two 32-in pumps from Fig. 11.7a are combined in parallel to deliver water at 60°F through 1500 ft of horizontal pipe. If $f = 0.025$, what pipe diameter will ensure a flow rate of 35,000 gal/min for $n = 1170$ r/min?
- P11.77** Two pumps of the type tested in Prob. 11.22 are to be used at 2140 r/min to pump water at 20°C vertically upward through 100 m of commercial-steel pipe. Should they be in series or in parallel? What is the proper pipe diameter for most efficient operation?
- P11.78** Suppose that the two pumps in Fig. P11.75 are modified to be in series, still at 710 r/min. What pipe diameter is required for BEP operation?
- P11.79** Two 32-in pumps from Fig. 11.7a are to be used in series at 1170 r/min to lift water through 500 ft of vertical cast-iron pipe. What should the pipe diameter be for most efficient operation? Neglect minor losses.

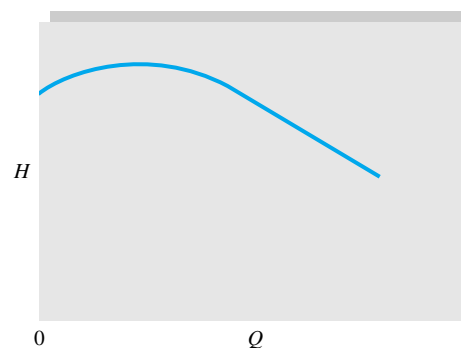
- P11.80** It is proposed to use one 32- and one 28-in pump from Fig. 11.7a in parallel to deliver water at 60°F. The system-head curve is $H_s = 50 + 0.3Q^2$, with Q in thousands of gallons per minute. What will the head and delivery be if both pumps run at 1170 r/min? If the 28-in pump is reduced below 1170 r/min, at what speed will it cease to deliver?

- P11.81** Reconsider the system of Fig. P6.68. Use the Byron Jackson pump of Prob. 11.28 running at 2134 r/min, no scaling, to drive the flow. Determine the resulting flow rate between the reservoirs. What is the pump efficiency?

- P11.82** The S-shaped head-versus-flow curve in Fig. P11.82 occurs in some axial-flow pumps. Explain how a fairly flat system-loss curve might cause instabilities in the operation of the pump. How might we avoid instability?



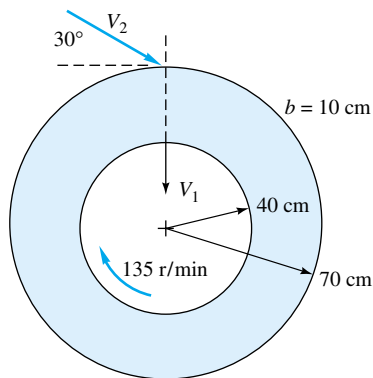
- P11.83** The low-shutoff head-versus-flow curve in Fig. P11.83 occurs in some centrifugal pumps. Explain how a fairly flat system-loss curve might cause instabilities in the operation of the pump. What additional vexation occurs when two of these pumps are in parallel? How might we avoid instability?



- P11.84** Turbines are to be installed where the net head is 400 ft and the flow rate 250,000 gal/min. Discuss the type, num-

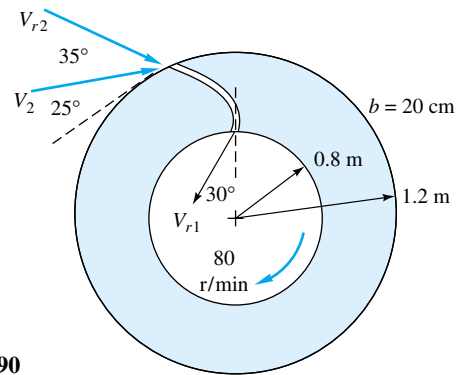
ber, and size of turbine which might be selected if the generator selected is (a) 48-pole, 60-cycle ($n = 150$ r/min) and (b) 8-pole ($n = 900$ r/min). Why are at least two turbines desirable from a planning point of view?

- P11.85** Turbines at the Conowingo Plant on the Susquehanna River each develop 54,000 bhp at 82 r/min under a head of 89 ft. What type of turbines are these? Estimate the flow rate and impeller diameter.
- P11.86** The Tupperware hydroelectric plant on the Blackstone River has four 36-in-diameter turbines, each providing 447 kW at 200 r/min and 205 ft³/s for a head of 30 ft. What type of turbines are these? How does their performance compare with Fig. 11.21?
- P11.87** An idealized radial turbine is shown in Fig. P11.87. The absolute flow enters at 30° and leaves radially inward. The flow rate is 3.5 m³/s of water at 20°C. The blade thickness is constant at 10 cm. Compute the theoretical power developed at 100 percent efficiency.



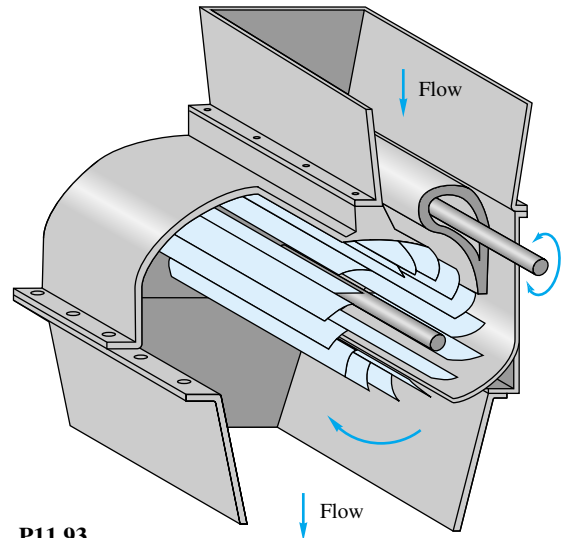
P11.87

- P11.88** A certain turbine in Switzerland delivers 25,000 bhp at 500 r/min under a net head of 5330 ft. What type of turbine is this? Estimate the approximate discharge and size.
- P11.89** A Pelton wheel of 12-ft pitch diameter operates under a net head of 2000 ft. Estimate the speed, power output, and flow rate for best efficiency if the nozzle exit diameter is 4 in.
- P11.90** An idealized radial turbine is shown in Fig. P11.90. The absolute flow enters at 25° with the blade angles as shown. The flow rate is 8 m³/s of water at 20°C. The blade thickness is constant at 20 cm. Compute the theoretical power developed at 100 percent efficiency.
- P11.91** The flow through an axial-flow turbine can be idealized by modifying the stator-rotor diagrams of Fig. 11.12 for energy absorption. Sketch a suitable blade and flow arrangement and the associated velocity diagrams. For further details see chap. 8 of Ref. 25.



P11.90

- P11.92** At a proposed turbine installation the available head is 800 ft, and the water flow rate is 40,000 gal/min. Discuss the size, speed, and number of turbines which might be suitable for this purpose while using (a) a Pelton wheel and (b) a Francis wheel.
- P11.93** Figure P11.93 shows a cutaway of a *cross-flow* or “Banki” turbine [55], which resembles a squirrel cage with slotted curved blades. The flow enters at about 2 o’clock, passes through the center and then again through the blades, leaving at about 8 o’clock. Report to the class on the operation and advantages of this design, including idealized velocity vector diagrams.

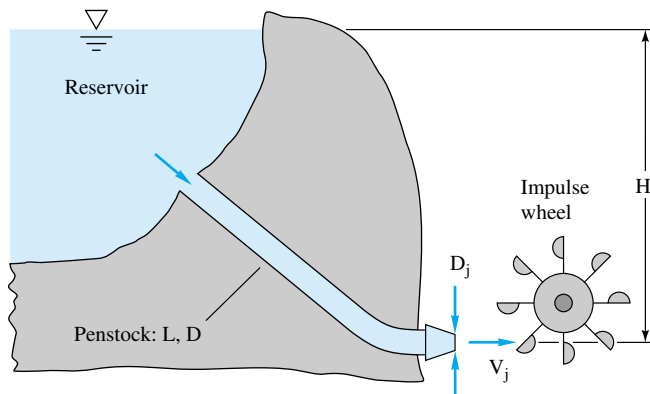


P11.93

- P11.94** A simple cross-flow turbine, Fig. P11.93, was constructed and tested at the University of Rhode Island. The blades were made of PVC pipe cut lengthwise into three 120°-arc pieces. When it was tested in water at a head of 5.3 ft and a flow rate of 630 gal/min, the measured power

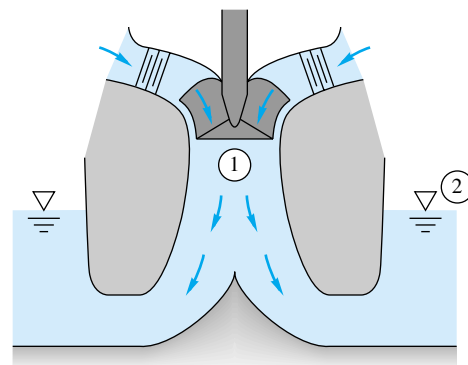
output was 0.6 hp. Estimate (a) the efficiency and (b) the power specific speed if $n = 200$ rev/min.

- P11.95** One can make a theoretical estimate of the proper diameter for a penstock in an impulse turbine installation, as in Fig. P11.95. Let L and H be known, and let the turbine performance be idealized by Eqs. (11.38) and (11.39). Account for friction loss h_f in the penstock, but neglect minor losses. Show that (a) the maximum power is generated when $h_f = H/3$, (b) the optimum jet velocity is $(4gH/3)^{1/2}$, and (c) the best nozzle diameter is $D_j = [D^5/(2fL)]^{1/4}$, where f is the pipe-friction factor.



P11.95

- P11.96** Apply the results of Prob. 11.95 to determining the optimum (a) penstock diameter and (b) nozzle diameter for the data of Prob. 11.92 with a commercial-steel penstock of length 1500 ft.
- P11.97** Consider the following nonoptimum version of Prob. 11.95: $H = 450$ m, $L = 5$ km, $D = 1.2$ m, $D_j = 20$ cm. The penstock is concrete, $\epsilon = 1$ mm. The impulse wheel diameter is 3.2 m. Estimate (a) the power generated by the wheel at 80 percent efficiency and (b) the best speed of the wheel in r/min. Neglect minor losses.
- P11.98** Francis and Kaplan turbines are often provided with *draft tubes*, which lead the exit flow into the tailwater region, as in Fig. P11.98. Explain at least two advantages in using a draft tube.
- P11.99** Turbines can also cavitate when the pressure at point 1 in Fig. P11.98 drops too low. With NPSH defined by Eq.



P11.98

(11.20), the empirical criterion given by Wislicenus [4] for cavitation is

$$N_{ss} = \frac{(r/\text{min})(\text{gal}/\text{min})^{1/2}}{[\text{NPSH}(\text{ft})]^{3/4}} \geq 11,000$$

Use this criterion to compute how high $z_1 - z_2$, the impeller eye in Fig. P11.98, can be placed for a Francis turbine with a head of 300 ft, $N_{sp} = 40$, and $p_a = 14$ lbf/in² absolute before cavitation occurs in 60°F water.

- P11.100** One of the largest wind generators in operation today is the ERDA/NASA two-blade propeller HAWT in Sandusky, Ohio. The blades are 125 ft in diameter and reach maximum power in 19 mi/h winds. For this condition estimate (a) the power generated in kW, (b) the rotor speed in r/min, and (c) the velocity V_2 behind the rotor.
- P11.101** A Darrieus VAWT in operation in Lumsden, Saskatchewan, that is 32 ft high and 20 ft in diameter sweeps out an area of 432 ft². Estimate (a) the maximum power and (b) the rotor speed if it is operating in 16 mi/h winds.
- P11.102** An American 6-ft diameter multiblade HAWT is used to pump water to a height of 10 ft through 3-in-diameter cast-iron pipe. If the winds are 12 mi/h, estimate the rate of water flow in gal/min.
- P11.103** A very large Darrieus VAWT was constructed by the U.S. Department of Energy near Sandia, New Mexico. It is 60 ft high and 30 ft in diameter, with a swept area of 1200 ft². If the turbine is constrained to rotate at 90 r/min, use Fig. 11.31 to plot the predicted power output in kW versus wind speed in the range $V = 5$ to 40 mi/h.

Word Problems

- W11.1** We know that an enclosed rotating bladed impeller will impart energy to a fluid, usually in the form of a pressure rise, but how does it actually happen? Discuss, with sketches, the physical mechanisms through which an impeller actually transfers energy to a fluid.
- W11.2** Dynamic pumps (as opposed to PDPs) have difficulty moving highly viscous fluids. Lobanoff and Ross [15] suggest the following rule of thumb: D (in) $> 0.015\nu/\nu_{\text{water}}$, where D is the diameter of the discharge pipe. For example, SAE 30W oil ($\approx 300\nu_{\text{water}}$) should

require at least a 4.5-in outlet. Can you explain some reasons for this limitation?

- W11.3** The concept of NPSH dictates that liquid dynamic pumps should generally be immersed below the surface. Can you explain this? What is the effect of increasing the liquid temperature?
- W11.4** For nondimensional fan performance, Wallis [20] suggests that the head coefficient should be replaced by $FTP/(\rho n^2 D^2)$, where FTP is the fan total pressure change. Explain the usefulness of this modification.
- W11.5** Performance data for centrifugal pumps, even if well scaled geometrically, show a decrease in efficiency with decreasing impeller size. Discuss some physical reasons why this is so.
- W11.6** Consider a dimensionless pump performance chart such as Fig. 11.8. What additional dimensionless parameters

might modify or even destroy the similarity indicated in such data?

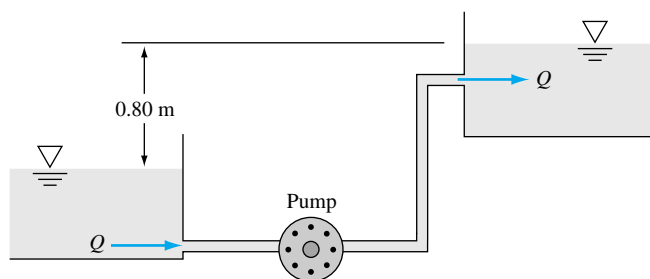
- W11.7** One parameter not discussed in this text is the *number of blades* on an impeller. Do some reading on this subject, and report to the class about its effect on pump performance.
- W11.8** Explain why some pump performance curves may lead to unstable operating conditions.
- W11.9** Why are Francis and Kaplan turbines generally considered unsuitable for hydropower sites where the available head exceeds 1000 ft?
- W11.10** Do some reading on the performance of the *free propeller* that is used on small, low-speed aircraft. What dimensionless parameters are typically reported for the data? How do the performance and efficiency compare with those for the axial-flow pump?

Comprehensive Problems

- C11.1** The net head of a little aquarium pump is given by the manufacturer as a function of volume flow rate as listed below:

$Q, \text{ m}^3/\text{s}$	$H, \text{ mH}_2\text{O}$
0	1.10
1.0 E-6	1.00
2.0 E-6	0.80
3.0 E-6	0.60
4.0 E-6	0.35
5.0 E-6	0.0

What is the maximum achievable flow rate if you use this pump to pump water from the lower reservoir to the upper reservoir as shown in Fig. C11.1? *Note:* The tubing is



C11.1

smooth with an inner diameter of 5.0 mm and a total length of 29.8 m. The water is at room temperature and pressure. Minor losses in the system can be neglected.

- C11.2** Reconsider Prob. 6.68 as an exercise in pump selection. Select an impeller size and rotational speed from the Byron Jackson pump family of Prob. 11.28 which will deliver a flow rate of $3 \text{ ft}^3/\text{s}$ to the system of Fig. P6.68 at minimum input power. Calculate the horsepower required.
- C11.3** Reconsider Prob. 6.77 as an exercise in turbine selection. Select an impeller size and rotational speed from the Francis turbine family of Fig. 11.21*d* which will deliver maximum power generated by the turbine. Calculate the turbine power output and remark on the practicality of your design.
- C11.4** A pump provides a net head H which is dependent on the volume flow rate Q , as follows: $H = a - bQ^2$, where $a = 80 \text{ m}$ and $b = 20 \text{ s}^2/\text{m}^5$. The pump delivers water at 20°C through a horizontal 30-cm-diameter cast-iron pipe which is 120 m long. The pressures at the inlet and exit of the system are the same. Neglecting minor losses, calculate the expected volume flow rate in gal/min.
- C11.5** In Prob. 11.23, estimate the efficiency of the pump in two ways: (a) Read it directly from Fig. 11.7*b* (for the dynamically similar water pump); and (b) Calculate it from Eq. (11.5) for the actual kerosene flow. Compare your results and discuss any discrepancies.

Design Project

D11.1 To save on electricity costs, a town water supply system uses gravity-driven flow from five large storage tanks during the day and then refills these tanks from 10 p.m. to 6 a.m. at a cheaper night rate of 7 ¢/kWh. The total resupply needed each night varies from 5 E5 to 2 E6 gal, with no more than 5 E5 gallons to any one tank. Tank elevations vary from 40 to 100 ft. A single constant-speed pump, drawing from a large groundwater aquifer and valved into five different cast-iron tank supply lines, does this job. Distances from the pump to the five tanks vary more or less evenly from 1 to 3 mi. Each line averages one elbow every 100 ft and has four butterfly valves which can be controlled at any desirable angle. Select a suitable pump family from one of the six data sets in this

chapter: Figs. 11.8, P11.24, and P11.31 plus Probs. 11.28, 11.35, and 11.38. Assume ideal similarity (no Reynolds-number or pump roughness effects). The goal is to determine pump and pipeline sizes which achieve minimum total cost over a 5-year period. Some suggested cost data are

1. Pump and motor: \$2500 plus \$1500 per inch of pipe size
2. Valves: \$100 plus \$100 per inch of pipe size
3. Pipelines: 50¢ per inch of diameter per foot of length

Since the flow and elevation parameters vary considerably, a random daily variation within the specified ranges might give a realistic approach.

References

1. D. G. Wilson, "Turbomachinery—From Paddle Wheels to Turbojets," *Mech. Eng.*, vol. 104, Oct. 1982, pp. 28–40.
2. D. Japikse and N. C. Baines, *Introduction to Turbomachinery*, Oxford University Press, New York, 1995.
3. D. W. Childs, *Turbomachinery Rotordynamics: Phenomena, Modeling, and Analysis*, Wiley, New York, 1993.
4. G. F. Wislicenus, *Fluid Mechanics of Turbomachinery*, 2d ed., McGraw-Hill, New York, 1965.
5. S. L. Dixon, *Fluid Mechanics and Thermodynamics of Turbomachinery*, 2d ed., Butterworth, London, 1998.
6. R. I. Lewis, *Turbomachinery Performance Analysis*, Wiley, New York, 1996.
7. E. S. Logan, Jr., *Turbomachinery: Basic Theory and Applications*, 2d ed., Marcel Dekker, New York, 1993.
8. A. J. Stepanoff, *Centrifugal and Axial Flow Pumps*, 2d ed., Wiley, New York, 1957.
9. J. W. Dufour and W. E. Nelson, *Centrifugal Pump Sourcebook*, McGraw-Hill, New York, 1992.
10. Sam Yedidiah, *Centrifugal Pump User's Guidebook: Problems and Solutions*, Chapman and Hall, New York, 1996.
11. T. G. Hicks and T. W. Edwards, *Pump Application Engineering*, McGraw-Hill, New York, 1971.
12. *Pump Selector for Industry*, Worthington Pump, Mountain-side, NJ, 1977.
13. R. Walker, *Pump Selection*, 2d ed., Butterworth, London, 1979.
14. R. H. Warring, *Pumps: Selection, Systems, and Applications*, 2d ed., Gulf Pub., Houston, TX, 1984.
15. V. L. Lobanoff and R. R. Ross, *Centrifugal Pumps, Design and Application*, Gulf Pub., Houston, TX, 1985.
16. H. L. Stewart, *Pumps*, 5th ed. Macmillan, New York, 1991.
17. A. B. McKenzie, *Axial Flow Fans and Compressors: Aerodynamic Design and Performance*, Ashgate Publishing, Brookfield, VT, 1997.
18. W. C. Osborne, *Fans*, 2d ed., Pergamon, London, 1977.
19. R. Jorgensen (ed.), *Fan Engineering*, Buffalo Forge, Buffalo, NY, 1983.
20. R. A. Wallis, *Axial Flow Fans and Ducts*, Wiley, New York, 1983.
21. H. P. Bloch, *A Practical Guide to Compressor Technology*, McGraw-Hill, New York, 1996.
22. H. Cohen et al., *Gas Turbine Theory*, Longman, London, 1996.
23. N. A. Cumpsty, *Compressor Aerodynamics*, Longmans, London, 1989.
24. G. C. Oates, *Aerothermodynamics of Gas Turbine and Rocket Propulsion*, 3d ed., AIAA, Washington, DC, 1998.
25. W. W. Bathe, *Fundamentals of Gas Turbines*, 2d ed., Wiley, New York, 1995.
26. J. Tong (ed.), *Mini-Hydropower*, Wiley, New York, 1997.
27. C. C. Warnick, *Hydropower Engineering*, Prentice-Hall, Englewood Cliffs, NJ, 1984.
28. J. J. Fritz, *Small and Mini Hydropower Systems*, McGraw-Hill, New York, 1984.
29. N. P. Cheremisinoff and P. N. Cheremisinoff, *Pumps/Compressors/Fans: Pocket Handbook*, Technomic Publishing, Lancaster, PA, 1989.
30. Hydraulic Institute, *Hydraulic Institute Standards for Centrifugal, Rotating, and Reciprocal Pumps*, New York, 1983.
31. I. J. Karassik, W. C. Krutzsch, W. H. Fraser, and J. P. Messina, *Pump Handbook*, 2d ed., McGraw-Hill, New York, 1985.
32. J. S. Gulliver and R. E. A. Arndt, *Hydropower Engineering Handbook*, McGraw-Hill, New York, 1990.

33. R. L. Daugherty, J. B. Franzini, and E. J. Finnemore, *Fluid Mechanics and Engineering Applications*, 8th ed., McGraw-Hill, New York, 1985.
34. R. H. Sabersky, A. J. Acosta, and E. G. Hauptmann, *Fluid Flow: A First Course in Fluid Mechanics*, 3d ed., Macmillan, New York, 1989.
35. J. P. Poynton, *Metering Pumps*, Marcel-Dekker, New York, 1983.
36. R. P. Lambeck, *Hydraulic Pumps and Motors: Selection and Application for Hydraulic Power Control Systems*, Marcel Dekker, New York, 1983.
37. T. L. Henshaw, *Reciprocating Pumps*, Van Nostrand Reinhold, New York, 1987.
38. J. E. Miller, *The Reciprocating Pump: Theory, Design and Use*, Wiley, New York, 1987.
39. D. G. Wilson, *The Design of High-Efficiency Turbomachinery and Gas Turbines*, 2d ed., Prentice-Hall, Upper Saddle River, N.J., 1998.
40. M. C. Roco, P. Hamelin, T. Cader, and G. Davidson, "Animation of LDV Measurements in a Centrifugal Pump," in *Fluid Machinery Forum—1990*, U.S. Rohatgi (ed.), FED, vol. 96, American Society of Mechanical Engineers, New York, 1990.
41. E. M. Greitzer, "The Stability of Pumping Systems: The 1980 Freeman Scholar Lecture," *J. Fluids Eng.*, vol. 103, June 1981, pp. 193–242.
42. B. Lakshminarayana, *Fluid Dynamics and Heat Transfer in Turbomachinery*, Wiley, New York, 1995.
43. L. F. Moody, "The Propeller Type Turbine," *ASCE Trans.*, vol. 89, 1926, p. 628.
44. H. H. Anderson, "Prediction of Head, Quantity, and Efficiency in Pumps—The Area-Ratio Principle," in *Performance Prediction of Centrifugal Pumps and Compressors*, vol. I00127, ASME Symp., New York, 1980, pp. 201–211.
45. B. Lakshminarayana and P. Runstadler, Jr. (eds.), "Measurement Methods in Rotating Components of Turbomachinery," *ASME Symp. Proc., New Orleans*, vol. I00130, 1980.
46. M. Murakami, K. Kikuyama, and B. Asakura, "Velocity and Pressure Distributions in the Impeller Passages of Centrifugal Pumps," *J. Fluids Eng.*, vol. 102, December 1980, pp. 420–426.
47. G. W. Koepl, *Putnam's Power from the Wind*, 2d ed., Van Nostrand Reinhold, New York, 1982.
48. R. L. Hills, *Power from Wind: A History of Windmill Technology*, Cambridge Univ. Press, Cambridge, 1996.
49. D. A. Spera, *Wind Turbine Technology: Fundamental Concepts of Wind Turbine Engineering*, ASME Press, New York, 1994.
50. A. J. Wortman, *Introduction to Wind Turbine Engineering*, Butterworth, Woburn, Mass., 1983.
51. F. R. Eldridge, *Wind Machines*, 2d ed., Van Nostrand Reinhold, New York, 1980.
52. D. M. Eggleston and F. S. Stoddard, *Wind Turbine Engineering Design*, Van Nostrand, New York, 1987.
53. M. L. Robinson, "The Darrieus Wind Turbine for Electrical Power Generation," *Aeronaut. J.*, June 1981, pp. 244–255.
54. D. F. Warne and P. G. Calnan, "Generation of Electricity from the Wind," *IEE Rev.*, vol. 124, no. 11R, November 1977, pp. 963–985.
55. L. A. Haimmerl, "The Crossflow Turbine," *Waterpower*, January 1960, pp. 5–13; see also *ASME Symp. Small Hydropower Fluid Mach.*, vol. 1, 1980, and vol. 2, 1982.
56. K. Eisele et al., "Flow Analysis in a Pump Diffuser: Part 1, Measurements; Part 2, CFD," *J. Fluids Eng.*, vol. 119, December 1997, pp. 968–984.